© 2014. Published by The Company of Biologists Ltd | Development (2014) 141, 1915-1926 doi:10.1242/dev.099432

RESEARCH ARTICLE

Clathrin heavy chain plays multiple roles in polarizing the *Drosophila* oocyte downstream of *Bic-D*

Paula Vazquez-Pianzola[1], Jacqueline Adam[1,*], Dominique Haldemann[1,*], Daniel Hain[1,*], Henning Urlaub[2] and Beat Suter[1,‡]

ABSTRACT

Bicaudal-D (Bic-D), Egalitarian (Egl), microtubules and their motors form a transport machinery that localizes a remarkable diversity of mRNAs to specific cellular regions during oogenesis and embryogenesis. Bic-D family proteins also promote dynein-dependent transport of Golgi vesicles, lipid droplets, synaptic vesicles and nuclei. However, the transport of these different cargoes is still poorly understood. We searched for novel proteins that either mediate Bic-D-dependent transport processes or are transported by them. Clathrin heavy chain (Chc) co-immunopurifies with Bic-D in embryos and ovaries, and a fraction of Chc colocalizes with Bic-D. Both proteins control posterior patterning of the *Drosophila* oocyte and endocytosis. Although the role of Chc in endocytosis is well established, our results show that *Bic-D* is also needed for the elevated endocytic activity at the posterior of the oocyte. Apart from affecting endocytosis indirectly by its role in *osk* mRNA localization, *Bic-D* is also required to transport *Chc* mRNA into the oocyte and for transport and proper localization of Chc protein to the oocyte cortex, pointing to an additional, more direct role of *Bic-D* in the endocytic pathway. Furthermore, similar to *Bic-D*, *Chc* also contributes to proper localization of *osk* mRNA and to oocyte growth. However, in contrast to other endocytic components and factors of the endocytic recycling pathway, such as Rabenosyn-5 (Rbsn-5) and Rab11, *Chc* is needed during early stages of oogenesis (from stage 6 onwards) to localize *osk* mRNA correctly. Moreover, we also uncovered a novel, presumably endocytosis-independent, role of *Chc* in the establishment of microtubule polarity in stage 6 oocytes.

KEY WORDS: Clathrin heavy chain, *Drosophila* oogenesis, RNA localization, Germ line, Microtubules, Polarity formation

INTRODUCTION

Studies in different organisms portray Bic-D homologs as factors that link the dynein-dynactin minus end-directed microtubule (MT) motor complex to different cargoes, moving them to particular cellular regions (Claussen and Suter, 2005; Vazquez-Pianzola and Suter, 2012). *Drosophila* Bic-D (also known as BicD) directly binds Egalitarian (Egl), which engages with Dynein light chain (Dlc; also know as Ctp) and specific mRNA localization signals (Navarro et al., 2004; Dienstbier et al., 2009). This complex is thought to associate with further proteins that regulate translation and stability of transported mRNAs, and the resulting larger complex translocates with the help of motors along the MT cytoskeleton. The Bic-D-dependent transport machinery is used repeatedly during *Drosophila* development. In oogenesis, *Bic-D* is needed for the transport of *osk*, *bcd* and *grk* mRNAs from the nurse cells into the oocyte and then to specific compartments within the oocyte (Suter and Steward, 1991; Ran et al., 1994; Clark et al., 2007). Correct localization of these factors within the oocyte is crucial for specifying anteroposterior and dorsoventral axes of oocytes and embryos. Later in the life cycle, the mRNA localization machinery delivers specific mRNAs to the apical side of the syncytial embryo (Bullock and Ish-Horowicz, 2001) and promotes localization of *inscuteable* mRNAs in neuroblasts (Hughes et al., 2004).

Drosophila Bic-D binds mRNA cargoes not only through the cargo-binding adaptor Egl, but also through the Fragile-X Mental Retardation Protein (Fmr1) (Bianco et al., 2010). Mammalian BicD2 regulates centrosome and nuclear positioning during mitotic entry (Splinter et al., 2010) and mammalian Bic-D isoforms bind Rab6 to control COPI-independent Golgi-endoplasmic reticulum transport (Matanis et al., 2002). Furthermore, Rab6B-BicD1 interaction regulates retrograde membrane transport in human neurites (Wanschers et al., 2007). Fly and worm *Bic-D* genes are also involved in nuclear migration in photoreceptors, oocytes and hypodermal precursor cells (Swan et al., 1999; Swan and Suter, 1996; Fridolfsson et al., 2010), and *Bic-D* also dynamically regulates transport of lipid droplets (Larsen et al., 2008). Given the involvement of Bic-D in the localization of surprisingly diverse cargoes, we searched for adaptor proteins that mediate cargo binding as well as for novel cargo molecules.

RESULTS

Chc associates with Bic-D in ovaries and embryos

Using two different monoclonal anti-Bic-D antibodies that recognize different epitopes, we immunopurified Bic-D complexes and identified Chc as a complex component in both approaches through mass spectrometry (Fig. 1A). Beads alone and beads coupled to control antibodies did not precipitate Chc. Myc-tagged Chc expressed under UAS control and a Flag-Tetracysteine (4C)-tagged Chc expressed from its endogenous promoter (Kasprowicz et al., 2008) were also immunoprecipitated with both anti-Bic-D antibodies from embryonic (Fig. 1B) and ovarian (Fig. 1C) extracts. Li et al. showed that Chc interacts directly with Bic-D and is its major interactor in the nervous system (Li et al., 2010). In contrast to this, Bic-D interacts with Egl, Chc, Pabp and others in embryos (Fig. 1A) (Vazquez-Pianzola et al., 2011; P.V.P. and B.S. unpublished data). Thus, in non-neuronal tissues, such as young embryos and ovaries, Chc appears to be one of many partners of Bic-D.

A fraction of Chc dynamically colocalizes with Bic-D in cortical regions of the oocyte

Anti-Bic-D antibody staining of ovaries that were fixed in a healthy state does not reveal aggregated structures, suggesting that native complexes are small particles that cannot be resolved with normal

[1]Institute of Cell Biology, University of Bern, 3012 Berne, Switzerland. [2]Bioanalytical Mass Spectrometry Group, Max Planck Institute for Biophysical Chemistry, 37077 Göttingen, Germany.
*These authors contributed equally to this work.

‡Author for correspondence (beat.suter@izb.unibe.ch)

Received 25 May 2013; Accepted 4 March 2014

Development (2014) 141, 1915-1926 doi:10.1242/dev.099432

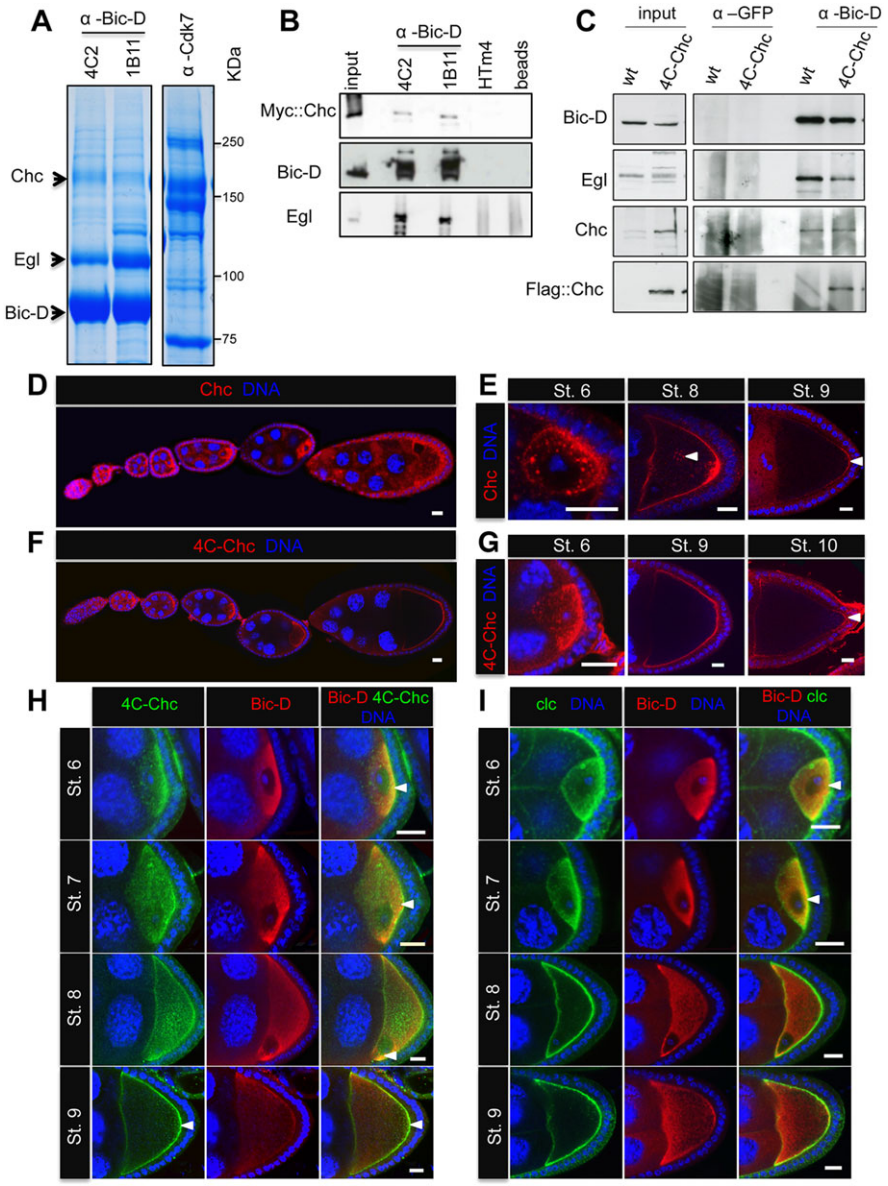

Fig. 1. Chc forms complexes with Bic-D in ovaries and embryos and is enriched in the oocyte. (A) Coomassie-stained SDS-PAGE showing anti-Bic-D IPs of total embryo extracts. Anti-Cdk7 antibodies were used as controls for nonspecific binding. Gel areas in which Chc, Bic-D and Egl were identified by mass spectrometry are indicated. Chc was identified in IPs performed with both anti-Bic-D antibodies, but was not found in the corresponding gel position after IPs with control antibodies. (B) IP of total embryo extracts expressing a Myc-tagged Chc expressed with the Nullo-Gal 4 driver. Antibodies used for IPs are indicated on top. Bic-D antibodies (4C2 and 1B11), a negative control mouse monoclonal antibody (HTm4) and beads alone were used. Western blots of the precipitated material were tested for the presence of Bic-D, Myc::Chc and Egl. (C) IPs with the antibodies indicated on top and input controls. Extracts were from ovaries of wild-type (wt) flies and from ovaries expressing a Flag-tagged Chc from the *4C-CHC* genomic construct. Anti-Bic-D (1B11) and anti-GFP antibodies were used. IP material was analyzed by western blot to check for the presence of Bic-D, Egl and Chc. Chc was detected with anti-Flag and with rabbit anti-mammalian Chc antibodies. (D) Immunostaining of wild-type ovaries with *Drosophila* anti-Chc antibody (red). (E) Enlarged view of the posterior part of stage 6, 8 and 9 egg chambers. Endogenous Chc is enriched in the oocyte in early stage egg chambers. Around stage 8, Chc localizes to the oocyte cortex and gets specifically enriched at the posterior pole. It becomes also concentrated in the center of the oocyte by stage 8 (arrowhead). At stage 9-10 it is enriched in the oocyte cortex and also at the posterior cortex (arrowhead). (F) Immunostaining of egg chambers expressing a Flag-tagged genomic Chc construct (*4C-Chc* transgene) with anti-Flag antibody (red) showing a similar germline staining as shown in D. Although 4C-CHC signal is reduced in follicle cells, the apparent Chc distribution pattern is very similar in the germ line, showing clear oocyte enrichment and a similar subcellular localization in the oocyte. Intensity differences appear to be due to different expression levels, nonspecific staining of the Chc antibody and penetration differences between antibodies. (G) Enlarged views of stage 6, 9 and 10 oocytes from F. Arrowhead indicates Chc enrichment at the posterior cortex. (H) Partial colocalization of Flag-tagged Chc (green) and Bic-D (red) is seen as yellow signal at the posterior cortex in stage 6-7 oocytes (arrowheads) and also at the anterior cortex at stage 8 (arrowhead), both known to be sites of action of Bic-D (Claussen and Suter, 2005). 4C-Chc enrichment at the posterior cortex is observed in stage 9 oocytes (arrowheads). (I) Immunostaining of wild-type ovaries with anti-Clc antibody (green) and anti-Bic-D antibody (red). Clc is also enriched in the oocyte. Partial Clc/Bic-D colocalization is also observed in stage 6-7 oocytes at the posterior cortex (arrowheads). However, Clc is more cortical and more uniformly distributed throughout the cortex in stage 8 egg chambers and no clear posterior enrichment is observed from stage 8 onwards. In D-I, ovarioles were also stained with Hoechst (blue) to visualize the DNA. Scale bars: 10 µm.

Development (2014) 141, 1915-1926 doi:10.1242/dev.099432

confocal microscopy. Colocalization studies can therefore only reveal whether Bic-D and Chc colocalized in the same cellular compartment. Indeed, a fraction of differently tagged (V5, Myc, Flag and GFP) or un-tagged Chc colocalizes with Bic-D in specific regions of the oocyte (Fig. 1D-H; data not shown). The germ line Chc signal became enriched in the oocyte from early stages onwards (Fig. 1D,F) and further signal enrichment became apparent at the posterior cortex of the oocyte from stage 6 onwards (Fig. 1E-G). During stage 6, Chc shows a partial colocalization with Bic-D and Egl at the posterior cortex (Fig. 1H; supplementary material Fig. S1). From stage 8-9 onwards, Chc signals localized to the oocyte cortex with higher enrichment at the posterior pole (Fig. 1E,G). Another partial colocalization between Bic-D/Egl and Chc is evident at the anterior cortex in stage 8 oocytes (Fig. 1H; supplementary material Fig. S1B).

As Clathrin activity in endocytosis involves also Clathrin light chain (Clc), we also studied Clc localization (Fig. 1I; supplementary material Fig. S1). Anti-Clc antibody staining also revealed Clc enrichment in the oocyte from early stages onwards. Clc concentrates at the posterior cortex, partially colocalizing with Bic-D in stage 6-7 oocytes. However, at stage 8, Clc is more uniformly distributed throughout the oocyte cortex and no clear posterior enrichment is observed from stage 8 onwards (Fig. 1I; supplementary material Fig. S1). Co-staining for Chc and Clc showed that, although both proteins are enriched in the oocyte and specifically at the oocyte cortex, they do not completely colocalize during development (supplementary material Fig. S1). This finding could suggest that Chc may play roles in oocyte development independently of Clc.

Bic-D localizes *Chc* mRNA to the oocyte and Chc protein to the posterior oocyte cortex

Bic-D and Egl seem to localize normally in Chc^{4} mutant ovarioles. The converse experiment, testing the function of *Bic-D* in later processes of oogenesis, is complicated by the fact that loss of *Bic-D* prevents oocyte formation (Ran et al., 1994). To deplete the germ line of Bic-D protein after oocyte determination, we used $Bic\text{-}D^{mom}$ flies in which *Bic-D* is provided solely from an inducible promoter that can be turned off once oocyte fate is established (Swan and Suter, 1996). Around 4 days after shutting down *Bic-D*, these ovaries contain mid-oogenesis germ line devoid of Bic-D. Once Bic-D protein became undetectable, Chc protein accumulation in the oocyte and at the

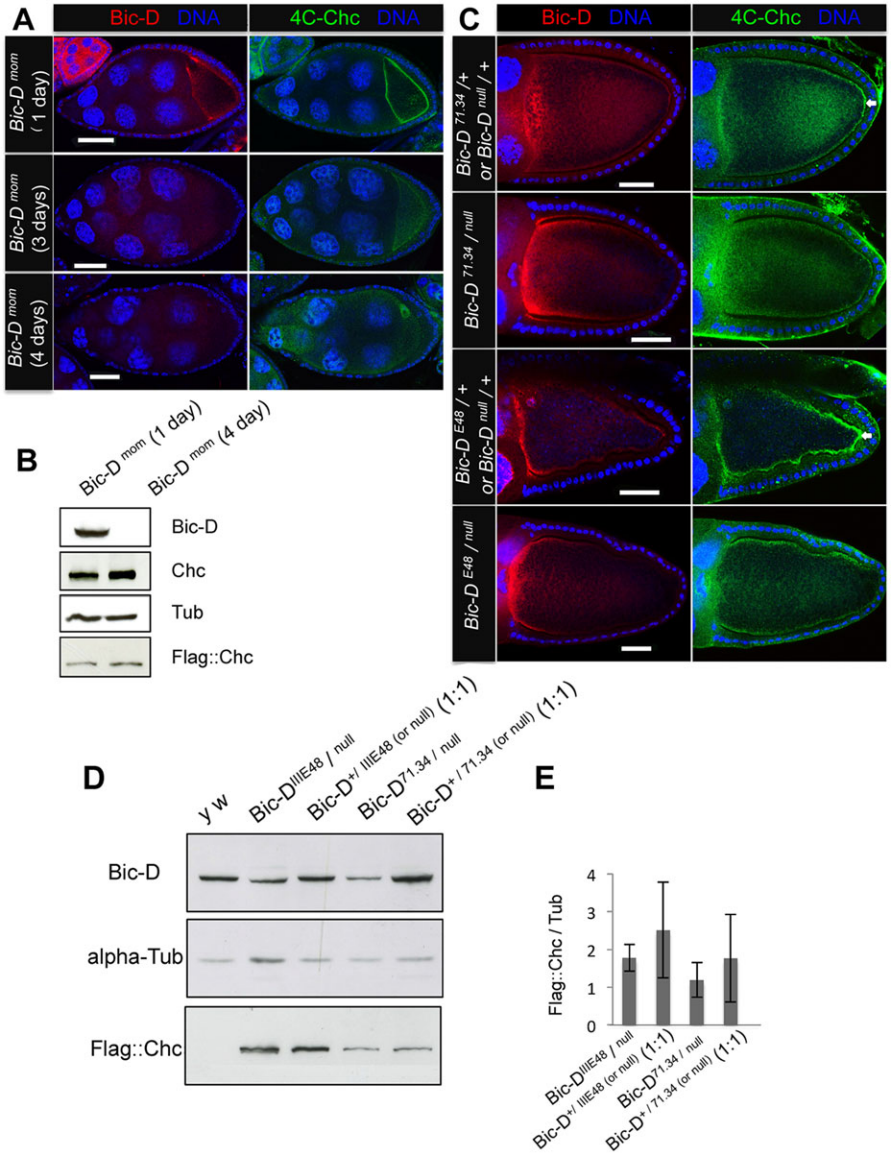

Fig. 2. Chc positioning at the oocyte cortex and at the oocyte posterior depends on *Bic-D*. (A) Egg chambers from $Bic\text{-}D^{mom}$ flies that express a copy of the *4C-Chc* transgene were immunostained for Bic-D (red) and for Chc using anti-Flag antibodies (green). Days after stopping Bic-D expression are indicated. The Flag signal around the oocyte nucleus is due to cross-reactivity of this antibody because it is also seen in wild-type ovaries stained with anti-Flag antibodies. (B) Western blots showing the levels of Bic-D, Chc, Flag-tagged Chc and α-Tubulin (Tub, loading control) in ovaries of the experiment shown in A. (C) Immunostainings were carried out as described for A. Heterozygous control egg chambers ($Bic\text{-}D^{null}$/+, $Bic\text{-}D^{71.34}$/+ or $Bic\text{-}D^{IIIE48}$/+) were randomly picked from the same cross as the test ovaries. Test ovaries with a dominant *Bic-D* allele ($Bic\text{-}D^{71.34}$/$Bic\text{-}D^{null}$ or $Bic\text{-}D^{IIIE48}$/$Bic\text{-}D^{null}$) showed reduced localization of Chc to the posterior cortex compared with the controls (arrowheads). (D) Levels of Bic-D, Flag-tagged Chc and α-Tubulin (loading control) in ovarian extracts of the experiment depicted in C were analyzed by western blotting with the corresponding antibodies. (E) Quantification of the levels of Flag::Chc relative to α-Tubulin from three independent western blot experiments described in D. Error bars represent s.d. of the measurements from the three blots. Scale bars: 30 µm.

Development (2014) 141, 1915-1926 doi:10.1242/dev.099432

oocyte cortex became reduced as well (Fig. 2A), even though Chc levels were not affected (Fig. 2B). Therefore, in the female germ line *Bic-D* acts upstream in localizing Chc.

The dominant mutant *Bic-D* alleles affect the localization of the cargo *osk* mRNA (Ephrussi et al., 1991; Kim-Ha et al., 1991). We therefore tested whether they also affect Chc localization. In stage 10 oocytes heterozygous for the dominant *Bic-D* alleles *Bic-D*^{IIIE48} or *Bic-D*$^{71.34}$ or *Bic-D*^{null}, Chc accumulated strongly at the posterior in most cases (79%, *n*=44 in *Bic-D*$^{71.34}$/+ or *Bic-D*^{null}/+; 89%, *n*=38 in *Bic-D*^{IIIE48}/+ or *Bic-D*^{null}/+). Thus, only 10-20% of oocytes with one normal copy of *Bic-D* showed reduced accumulation of Chc at the posterior. By contrast, posterior accumulation of Chc was reduced in 49% (*BicD*^{IIIE48}/*Bic-D*^{null}; *n*=49) and 44% (*Bic-D*$^{71.34}$/*Bic-D*^{null}; *n*=99) of the mutant stage 9-10 oocytes (Fig. 2C). Interestingly, the observed effects are not due to an abolished interaction between Chc and the dominant mutant Bic-D protein because Chc is efficiently precipitated with Bic-D from *Bic-D*^{IIIE48}/*Bic-D*^{null} and *Bic-D*$^{71.34}$/*Bic-D*^{null} mutant extracts (not shown). Furthermore, Chc protein levels are also normal in these ovaries (Fig. 2D,E). Because a significant portion of dominant Bic-D mutant protein accumulates strongly at the anterior cortex, it appears that there may not be sufficient functional Bic-D available to transport Chc cargo to the posterior cortex.

Because *Bic-D* transports mRNAs into the oocyte, we analyzed the distribution of *Chc* mRNA in wild-type and *Bic-D*^{mom} ovaries (Fig. 3A,B). Once the female germ line was depleted of Bic-D, *Chc* mRNA accumulation in the oocyte also became reduced, even though total levels of *Chc* mRNA remained normal (Fig. 3C). *Bic-D* thus functions to localize *Chc* mRNA into the oocyte, rather than in stabilizing the transcript. Similar to the mRNA levels, ovarian Chc protein levels were also normal in *Bic-D*^{mom} mutants (Fig. 2B).

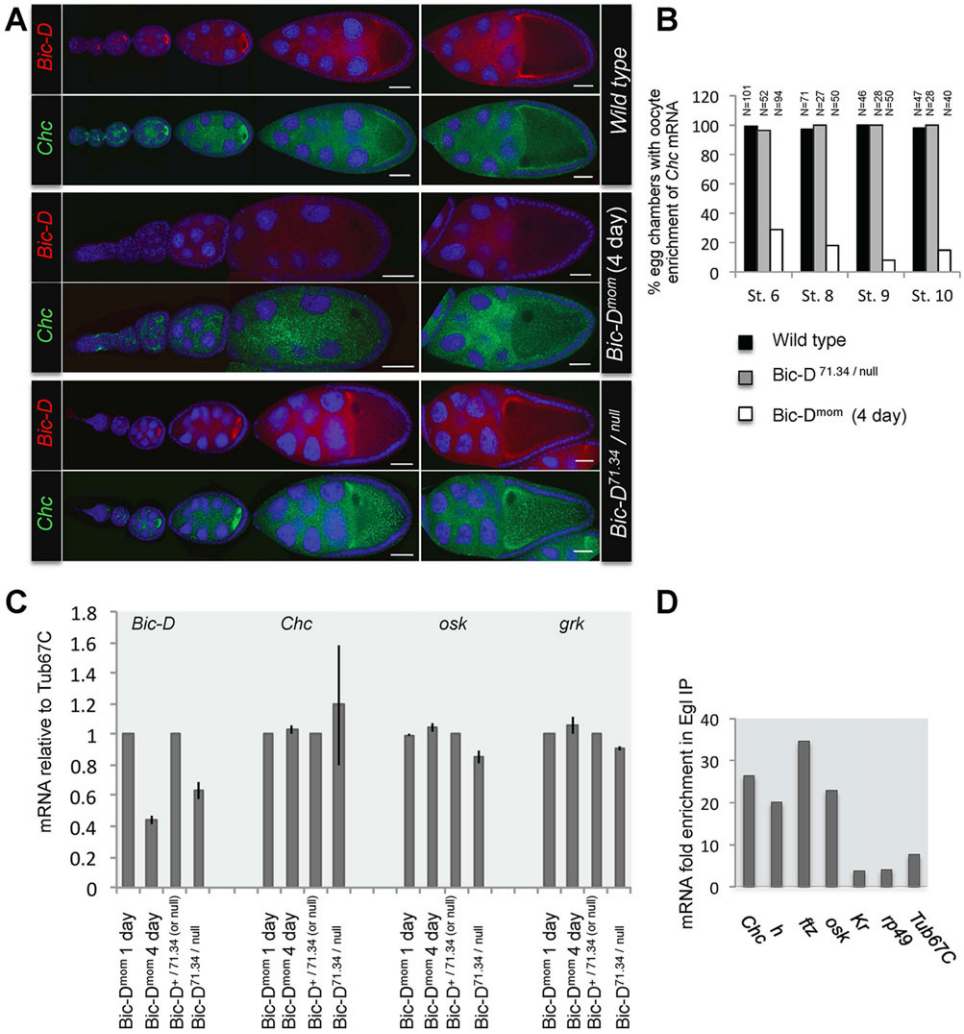

Fig. 3. *Chc* mRNA is transported into the oocyte by the Bic-D/Egl machinery. (A) *In situ* hybridization to *y w* controls (upper panels), to egg chambers 4 days after turning off *Bic-D* expression (*Bic-D*^{mom}, middle panels) and to *Bic-D*$^{71.34}$/*Bic-D*^{null} egg chambers (lower panels) showing *Bic-D* mRNA (red) and *Chc* mRNA (green). *Chc* mRNA fails to efficiently accumulate in *Bic-D*^{mom} oocytes lacking *Bic-D* mRNA. Oocytes are on the right side of each egg chamber. *Chc* mRNA still accumulates in *Bic-D*$^{71.34}$/*Bic-D*^{null}oocytes. (B) Quantification of the number of egg chambers showing oocyte enrichment of *Chc* from the experiment described in A. (C) Levels of *Bic-D*, *Chc*, *osk*, *grk* and *Tub67C* mRNA in ovaries as measured by qRT-PCR 1 day (when Bic-D levels are still normal) and 4 days after shutting down *Bic-D* expression. A 1:1 mixture of heterozygous dominant mutants (+/*Bic-D*$^{71.34}$) and heterozygous null mutants (+/*Bic-D*^{null}) was used as control for *Bic-D*$^{71.34}$/*Bic-D*^{null}; values were normalized to *Tub67C* levels and fold change calculated from two independent biological samples using the Pfaffl method (Pfaffl, 2001). Bars show the average fold change and the lines show the maximum and minimum values. Results with two other samples and analysis by semi-quantitative PCR showed similar results (not shown). *Chc* transcripts are stable in egg chambers 4 days after shutting down *Bic-D* and at a time when *Bic-D* mRNAs are clearly reduced. (D) Wild-type embryo extracts (control IP) and extracts expressing an Egl::GFP fusion protein were subject to immunoprecipitation using anti-GFP antibodies. qPCR was used to assay the presence of *Chc* mRNA, known localized mRNAs (*h*, *ftz*, *osk*) and negative controls (*Kr*, *rp49*, *Tub67C*). The values represent the average of two IPs for each treatment. qPCR for all samples were performed in triplicate. Scale bars: 30 µm.

Development (2014) 141, 1915-1926 doi:10.1242/dev.099432

Reduced oocyte accumulation of Chc protein in Bic-D-depleted egg chambers therefore seems to be due to the lack of *Chc* mRNA transport. To test whether the Bic-D/Egl localization machinery associates with *Chc* mRNA, we immunopurified Bic-D/Egl::GFP complexes. This procedure resulted in enrichment of *Chc* mRNAs to a similar level as the enrichment of the known Bic-D/Egl targets *ftz*, *hairy* and *osk* (Fig. 3D). By contrast, *Kr*, a non-localizing mRNA, and the housekeeping mRNAs *rp49* (also know as RpL32) and *Tub67C* were much less enriched in these immunoprecipitates.

Because Bic-D is involved in localizing *Chc* mRNA and protein, it became important to assess the dynamics of Chc::GFP transport in the presence and absence of *Bic-D* in the female germ line (Fig. 4). As seen for Chc in fixed samples, Chc::GFP accumulates at the oocyte cortex in the wild type, but much less so in *Bic-D*^{mom} oocytes (Fig. 4A). Chc::GFP spots move in strictly linear directions in mutant and wild-type oocytes, suggesting that Chc::GFP is transported along MT tracks. Clusters of similar size and shape to the moving spots are located in the vicinity of the cortex in *Bic-D*^{mom} oocytes (Fig. 4B) but not in wild-type oocytes, in which the strong accumulation of cortical Chc::GFP leads to a more homogenous and brighter signal (Fig. 4B). Particles moved frequently and with similar directionality along the oocyte cortex in wild type and mutants (Fig. 4C,D), but average particle speed was significantly higher in mutants (Fig. 4E). It therefore seems that lack of Bic-D affects movement of Chc on MTs and that this defect prevents cortical accumulation of Chc protein. The increased particle speed observed upon loss of *Bic-D* may point towards an inhibitory function of Bic-D and dynein-mediated transport towards kinesin-based transport. Interestingly, the particle speed for Rab6, another Bic-D cargo, increases also after inhibition of the dynein-dynactin interaction by expressing p50-dynamitin (Januschke et al., 2007). Furthermore, overexpression of *Chc::GFP* in the hypomorphic and the dominant *Bic-D* mutant background enhanced the *Bic-D*-dependent *osk* mislocalization phenotypes. Different cargoes competing for limited Bic-D could lead to such an enhancement of the hypomorphic phenotype. Alternatively, Chc overexpression could modify the cortex in a way that improves anchoring of ectopic *osk* mRNA (supplementary material Fig. S2).

Like *Bic-D*, *Chc* is needed for proper localization of *osk* mRNA and for oocyte growth

Although *Chc*^{1}, *Chc*^{2} and *Chc*^{3} are lethal alleles, *Chc*^{4} is a non-lethal mutant allele that causes a remarkable reduction in endocytic capacity and a wide range of phenotypes, including sterility (Bazinet et al., 1993; Peralta et al., 2009). In homozygous, hemizygous and transheterozygous (*Chc*^{1}/*Chc*^{4}) *Chc*^{4} females, oogenesis arrests mostly at stage 8, but escaper follicles develop into eggs. This *Chc*^{4} oogenesis arrest phenotype is rescued by different *Chc*$^{+}$ constructs, revealing also that differently tagged transgenes had *Chc*$^{+}$ rescuing activity. A single genomic copy of *Chc*$^{+}$ with a Flag-tag (*4C-Chc*) (Kasprowicz et al., 2008) rescued sterility, poor viability and locomotive defects of *Chc*^{1}/*Chc*^{4} females, and two copies of this transgene also rescued *Chc*^{1} lethality. *pUASP-Chc-V5*, *pUASP-Chc::eGFP* (Li et al., 2010) and *pUASP-myc-Chc*, driven by an *Actin-Gal4* driver, were able to rescue the sub-lethality and sterility of *Chc*^{4}/*Chc*^{1} females, but not the *Chc*^{1} lethality. The reduced rescue efficiency could be due to low or non-ubiquitous expression of the Gal4 driver or the pUASP vector. *Chc*^{4} mutant egg chambers showed an overall reduced size, smaller oocytes and smaller, but normally localized, oocyte nuclei (Fig. 5A). Receptor-mediated endocytic yolk uptake into the oocyte depends on Clathrin and is initiated normally around stage 8 (Tanaka et al., 2011). *Chc*^{4} mutant oocytes and mutant larval Garland cells showed reduced endocytosis (Peralta et al., 2009) (data not shown).

In *Chc*^{4} mutants, maternal mRNAs seemed to be imported normally from the nurse cells into the oocyte and *grk*, *orb*, *Bic-D* and *Chc* mRNAs showed mostly normal localization (Fig. 5B). By contrast, *osk* mRNA accumulated in oocytes, but it was found uniformly distributed in *Chc*^{4} mutant oocytes or ectopically localized in the middle of stage 9-10 oocytes unless a rescue transgene was provided (Fig. 5C). *osk* mRNA localization at the anterior and posterior cortex of stage 8 oocytes was mostly not observed in mutant egg chambers. Osk protein levels remain low in *Chc*^{4} stage 9 egg chambers, and 12 out of 20 egg chambers did not show Osk expression at the posterior cortex compared with only three out of 20 in the wild type (data not shown). Germ line clones of the lethal allele *Chc*^{GF23} (Yan et al., 2009) showed morphological defects, but, nevertheless, *grk* mRNA localization was mostly normal (Fig. 6A). By contrast, *osk* mRNA failed to enrich at the oocyte posterior from stage 6 onwards (Fig. 6B), further supporting the view that *Chc* is needed more specifically for proper localization of *osk* mRNA.

Chc organizes oocyte MT polarity already before bulk endocytosis starts

Mutations in *Rab11* and *Rabenosyn-5* (*Rbsn-5*), two genes involved in endocytosis, cause defects in *osk* mRNA localization

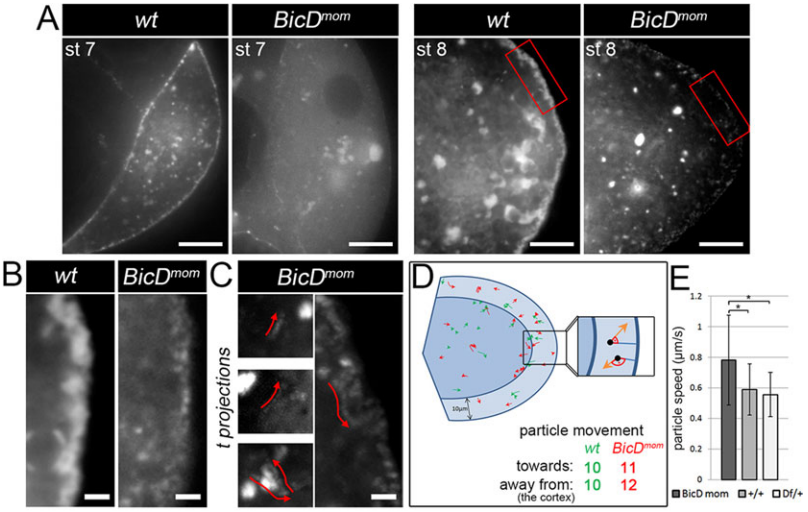

Fig. 4. Dynamics of Chc::GFP movement depends on *Bic-D*. (A) Chc::GFP was expressed under the control a maternal tubulin Gal4 driver in wild-type and *BicD*^{mom} egg chambers. *BicD*^{mom} and control flies were observed 5 days after shutting off *Bic-D*. Oocytes in stage 7 (left) and stage 8 (right) are shown. Chc::GFP is strongly enriched at the cortex in the wild type, but not in *BicD*^{mom} oocytes. (B) Magnified views of the posterior oocyte regions (indicated by red boxes in A). (C) Examples of Chc::GFP transport particles moving along linear tracks. Superposition of frames over time (100 s) makes moving particles appear as a string of faint dots (indicated by red arrows next to the string) within the oocyte (left three panels) and at the oocyte cortex (right panel). (D) Overview of the directionality of Chc::GFP particle movement in wild-type (green) and *BicD*^{mom} (red) oocytes from two oocytes per genotype. Particles within a distance of 10 µm from the cortex were grouped dependent on the angle between their track and the shortest distance to the cortex (0-90°: towards the cortex, >90°: away from cortex). (E) Speed of particle movement in wild-type, *Df(2L)Exel7068*/+ and *BicD*^{mom} oocytes; n=30, 13, 12, respectively; error bars represent s.d.; $P \leq 0.05$. Scale bars: 10 µm (A); 2 µm (B,C).

Development (2014) 141, 1915-1926 doi:10.1242/dev.099432

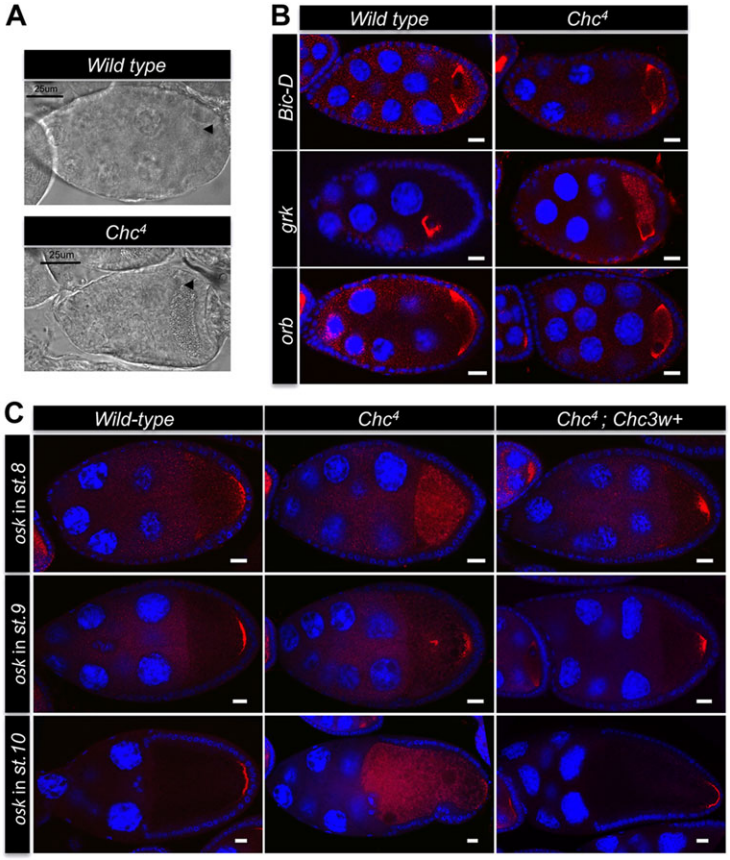

Fig. 5. *Chc* is essential during oogenesis and, like *Bic-D*, is needed for proper localization of *osk* mRNA. (A) Phase contrast image of a wild-type and a Chc^4 mutant egg chamber displaying reduced growth. Arrowhead indicates oocyte nucleus position. Posterior is to the right. (B) *In situ* hybridization to whole-mount wild-type egg chambers (left panels) and those of Chc^4 mutants (right panels) showing the RNAs indicated [red; DNA (Hoechst) in blue]. mRNAs localize normally, although *grk* produces an additional diffuse signal in the oocyte. (C) *osk* mRNA (red) localization to the posterior oocyte cortex is impaired in stage 8-10 Chc^4 mutant egg chambers, but rescued by a genomic wild-type Chc^+ construct (*Chc3w+*; right panels). Note the central accumulation in the mutant stage 9 oocyte. Scale bars: 25 µm (A); 10 µm (B,C).

(Jankovics et al., 2001; Dollar et al., 2002; Tanaka and Nakamura, 2008). However, as opposed to *Rab11* and *Rbsn-5*, Chc^4 affects *osk* mRNA localization earlier than stage 9. We therefore tested whether problems in MT organization in Chc^4 egg chambers could lead to *osk* mRNA mislocalization (Fig. 7). Indeed, Kinesin heavy chain (Khc), a marker for stable MT plus ends, is enriched at the posterior cortex only in wild-type oocytes and in rescued mutants, but not in Chc^4 mutants (Fig. 7A). Posterior enrichment of EB1, a marker for growing MT plus ends, was also affected in stage 6-9 Chc^4 mutant egg chambers (Fig. 7B). Furthermore, α-Tubulin staining showed that MTs are enriched at the posterior oocyte cortex at stage 6, before they re-focus at the anterior and anterodorsal cortex by stage 8 (Fig. 7C). In Chc^4 mutant egg chambers, α-Tubulin shows either a dotted pattern or no staining at the posterior cortex in stage 6. Also, stage 8 oocytes do not show anterior α-Tubulin accumulation, indicating again problems in focusing the MT network. In agreement, focusing of MTs was also not observed in germline clones of the Chc^{GF23} allele (supplementary material Fig. S3). Such early functions in MT organization were not described for other genes involved in the endocytic pathway (Jankovics et al., 2001; Dollar et al., 2002; Tanaka and Nakamura, 2008). Revisiting *Rbsn-5* and *Rab5* mutant phenotypes in our laboratory, we confirmed normal localization of Khc in early oogenesis and that Khc localization was only affected after stage 9 (supplementary material Fig. S4). Therefore, *Rbsn-5* and *Rab5* (involved in the formation of early endosomes) mutations that interfere with endocytosis, affect MT organization only after stage 9 of oogenesis. By contrast, *Chc* is involved already earlier, around stage 6, in the organization of MT polarity and the MT network. Because bulk endocytosis starts only after MT reorganization at stage 8 and because the other endocytic genes tested are not important for MT organization prior to stage 9, it appears that *Chc* may play an endocytosis-independent role in MT organization around stage 6. Interestingly, in germ lines lacking Bic-D, Khc is also delocalized and detached from the posterior cortex (Fig. 7D) and α-Tubulin staining revealed abnormal MT organization (data not shown). Even though the defects observed in *Chc* mutants are clearly stronger than the ones observed in the hypomorphic $Bic\text{-}D^{mom}$ situation, this result indicates that, like *Chc*, *Bic-D* is also involved in controlling MT organization.

Chc links Bic-D to the regulation of the endocytic pathway and posterior patterning

Clathrin plays a major role in the formation of coated vesicles during endocytosis. As Bic-D interacts with Chc and is needed for proper localization of Chc in oocytes (Figs 1, 2), we analyzed the levels of endocytosis in $BicD^{mom}$ egg chambers by visualizing FM4-64 uptake and autofluorescence of yolk granules (Fig. 8A,B). Wild-type stage 8-9 egg chambers show an accumulation of FM4-64 in the follicle cells and at the oocyte cortex with a higher accumulation at the posterior (Fig. 8A). Similarly, yolk granules accumulate at high amounts and are clearly enriched at the posterior in wild-type oocytes (Fig. 8A). However, in $Bic\text{-}D^{mom}$ egg chambers in which Bic-D has become undetectable (labeled 'day 4'), FM4-64 dye uptake and yolk granule autofluorescence are reduced and mostly lack enrichment at the posterior cortex (Fig. 8A,B). Therefore, *Bic-D* is needed to support oocyte endocytosis. Elevated levels of posterior endocytosis have been linked to the establishment of posterior identity (Vanzo et al., 2007; Tanaka and Nakamura, 2008). To find out whether the Bic-D-mediated elevated accumulation of Chc at the posterior cortex can be linked to the elevated endocytosis at the posterior pole, we took

Development (2014) 141, 1915-1926 doi:10.1242/dev.099432

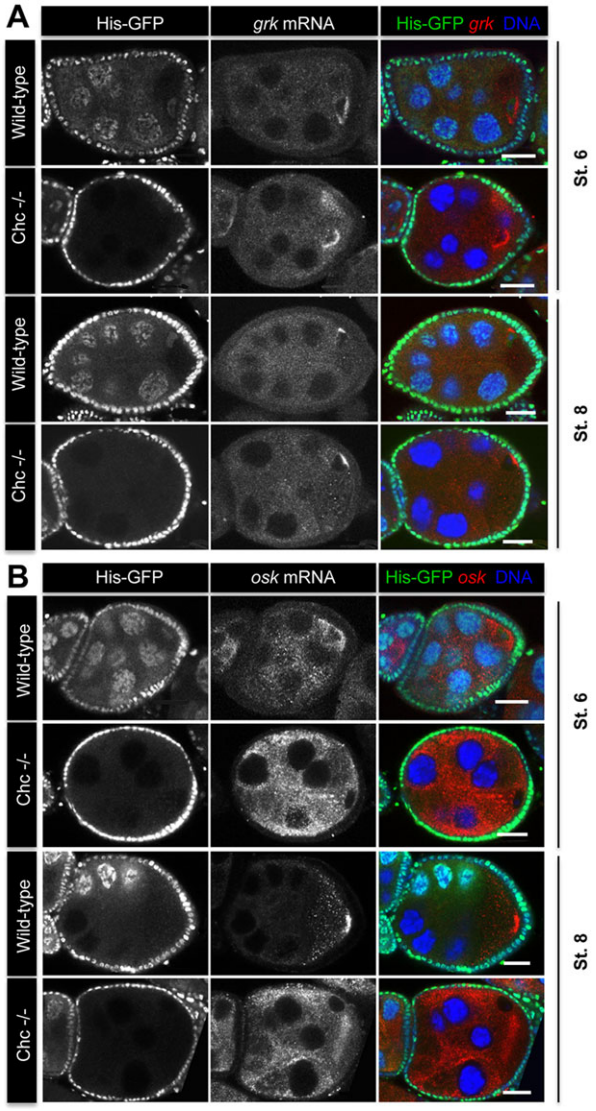

Fig. 6. *osk* mRNA localization is affected in Chc^{null} germline clones. Chc^{GF23} germline clones marked by the absence of nuclear GFP signal (green). (A) *grk* mRNA (red) is enriched at the posterior in stage 6 egg chambers in wild-type and mutant clones. At stage 7-8, *grk* mRNA is found at the anterior dorsal side of the nucleus. (B) *osk* mRNA (red) is enriched in the oocyte and at the posterior during early oogenesis (up to stage 6). Although *osk* mRNA is enriched at the posterior in early Chc^{GF23} mutant clones (not shown), posterior enrichment is lost by stage 6 in Chc^{GF23} mutants. Blue staining (Hoechst) shows the DNA. Scale bars: 20 μm.

advantage of a dominant *Bic-D* allele that prevents this elevated accumulation of Chc at the posterior pole. In $Bic\text{-}D^{71.34}/Bic\text{-}D^{null}$ oocytes, FM4-64 dye uptake is also reduced (Fig. 8A). In addition, these oocytes show reduce yolk granule autofluorescence and, although they still show more yolk granules towards the posterior, these granules are smaller and not clearly enriched at the very posterior cortex where they concentrate in wild-type oocytes (Fig. 8A,B). Interestingly, in synapses lacking functional Chc small vesicles fail to be formed and these synapses contain larger vesicles (Kasprowicz et al., 2008) This is consistent with Bic-D-dependent posterior localization of its interaction partner Chc being an essential step in upregulating posterior endocytosis and patterning. Similarly, the absence of Bic-D and the presence of the $Bic\text{-}D^{71.34}$ mutation interfere with posterior oocyte localization of Rab11 and Rbsn-5 (Fig. 8C,D).

DISCUSSION

Chc and Bic-D are present in the same complexes in embryos and ovaries, where their functions show considerable overlap. As opposed to the nervous system, in which Li et al. describe Chc as the major Bic-D-associated protein in *Drosophila* heads (Li et al., 2010), we found that Chc is one of many Bic-D partners in ovaries and embryos. The magnitude of these differences suggests that they are not solely caused by the different purification protocols employed. Instead, they seem to reflect differences in tissue-specific complex formation and additional activities of Bic-D during oogenesis and embryogenesis that are mediated by different adaptor and cargo proteins.

Dual role of Bic-D in stimulating endocytosis at the posterior pole of the oocyte

Chc is the main structural component of clathrin-coated pits and vesicles, and a central player in clathrin-mediated endocytosis (Brodsky, 2012; Faini et al., 2013). The association of Bic-D with Chc led us to discover that *Bic-D* is needed for endocytosis in the oocyte through two different mechanisms. On one hand, Bic-D seems to localize *Chc* mRNA into the oocyte. But in addition, Bic-D also appears to transport Chc protein to the posterior oocyte cortex. In *Bic-D* dominant mutants *Chc* mRNA localization is normal, but Chc protein is reduced at the posterior and much Bic-D protein remains anteriorly, pointing to insufficient protein transport towards posterior. Direct observation of moving particles also show that lack of Bic-D alters the dynamics of Chc::GFP transport in oocytes.

Li and co-workers proposed that Bic-D is needed for localization of Chc to periactive zones through a role in synaptic vesicle recycling (Li et al., 2010). A Chc recycling mechanism may be at work at the oocyte cortex, but our data are also consistent with a function of Bic-D in transporting Chc to the oocyte and then to its cortex. It seems possible that both mechanisms are at work in the female germ line, but further studies are needed to clarify their individual contribution and to find out whether they occur simultaneously or successively.

Endocytosis-independent function of Chc in establishing MT polarity

From oogenesis stage 8 on, *Chc* also functions in posterior localization of *osk* mRNA. However, as opposed to Bic-D and Egl, Chc does not get recruited to localizing mRNAs injected into syncytial embryos (data not shown), suggesting a more indirect role in mRNA transport. At stage 6, slightly before *osk* mRNA localization defects become visible, Chc is involved in organizing the MTs that are needed for setting up anteroposterior oocyte polarity. By contrast, *Rbsn-5* and *Rab11*, encoding components of the endocytic and endocytic recycling pathway, respectively, are involved in *osk* mRNA localization only at stage 9 (Jankovics et al., 2001; Dollar et al., 2002; Tanaka and Nakamura, 2008) and *Rbsn-5* and *Rab-5* null mutants show MT polarity defects also only after stage 9 (Tanaka and Nakamura, 2008) (supplementary material Fig. S4). Therefore, although many endocytosis-related genes play roles later in oogenesis for MT maintenance, *Chc* is needed for the establishment of MT organization already around oogenesis stage 6. Furthermore, establishment of MT polarity by *Chc* appears to be endocytosis independent because $Rbsn\text{-}5^{null}$ mutant egg chambers (showing strong endocytosis defects) and $Rab\text{-}5^{null}$ mutants (also required for vesicle fusion in early endocytosis) do not reveal a requirement for this process (Tanaka and Nakamura, 2008; Morrison et al., 2008) (supplementary material Fig. S4).

Interestingly, mammalian Chc (CHC17; also known as CLTC) associates with mitotic spindles and forms a complex with the

Development (2014) 141, 1915-1926 doi:10.1242/dev.099432

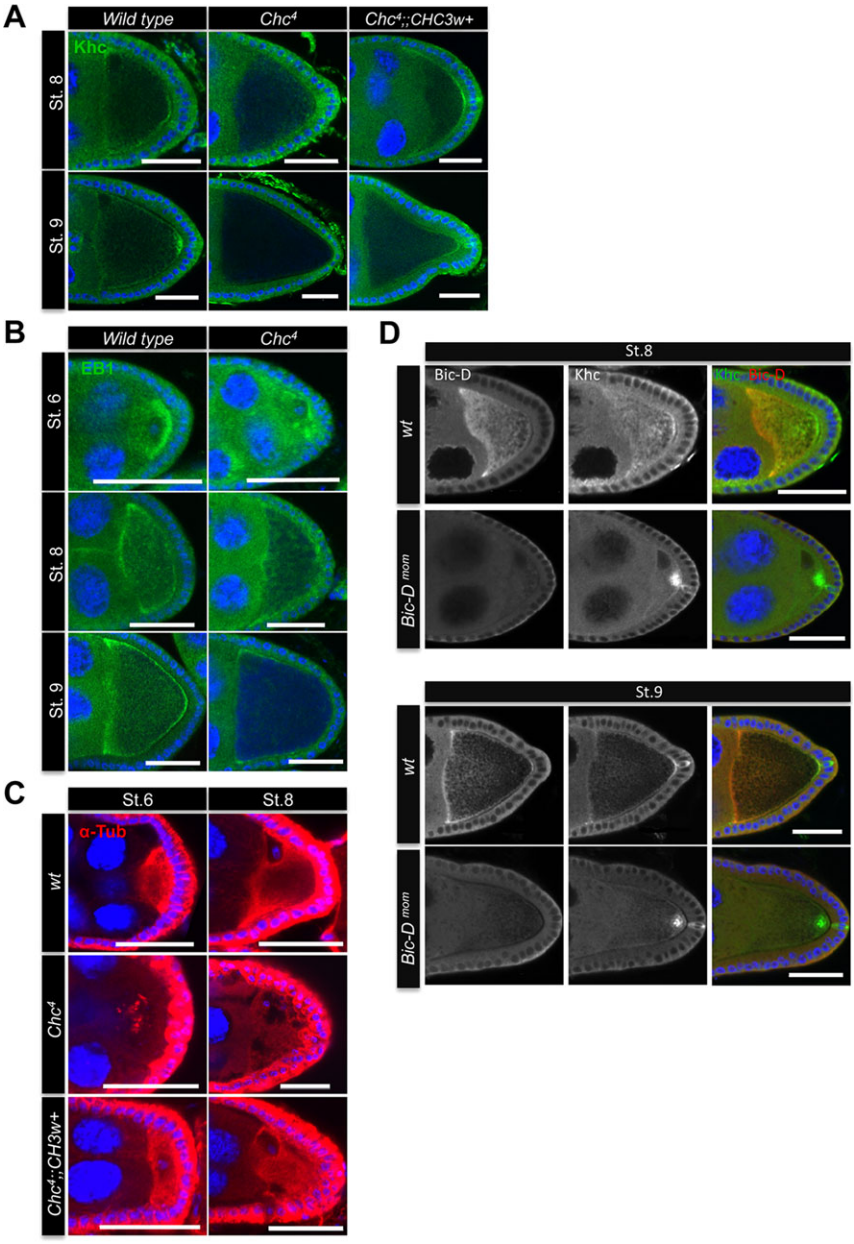

Fig. 7. *Chc* and *Bic-D* are needed to organize MT polarity in the oocyte. (A) Immunostaining with anti-Khc antibodies (green) shows posterior Khc localization in wild-type and rescued oocytes, but not in Chc^4 mutants. (B) Detection of the growing plus end MT marker EB1 by immunostaining (green) shows lack of posterior cortex enrichment in Chc^4. (C) Immunostaining with anti-α-Tubulin antibodies (red) shows MTs focusing on the posterior oocyte cortex at stage 6 and on the anterior cortex in stage 8. This pattern requires a Chc^+ copy. (D) Wild-type and $Bic\text{-}D^{mom}$ (3-4 days after Bic-D expression was shut off) egg chambers immunostained for Bic-D (red) and for Khc (green) showed strong Khc enrichment along the posterior cortex only in the presence of Bic-D. In $Bic\text{-}D^{mom}$, a posterior Khc dot is detected detached from the cortex. Scale bars: 30 μm.

MT-associated proteins TACC3 and ch-TOG (also known as CKAP5) (Royle et al., 2005; Booth et al., 2011). This complex stabilizes kinetochore fibers by mediating short-distance interactions between adjacent MTs (Booth et al., 2011). Similar to *Chc*, *Drosophila* ch-TOG, encoded by *mini spindles* (*msps*), is also required for organization and structure of oocyte MTs and for the mRNA localization of *bicoid* (*bcd*) mRNA (Moon and Hazelrigg, 2004). However, the hypomorphic *msps* mutants did not show defects in *osk* mRNA localization. Stronger reduction of *msps* activity may help in determining whether the hypomorphic *msps* mutants still provide sufficient *msps* activity to localize *osk* mRNA or whether the roles of *Chc* in MT organization and *osk* mRNA localization can be separated. Chc-coated vesicles also form at the trans-Golgi network (TGN). Interestingly, non-centrosomal MTs nucleating at the Golgi have been found to be indispensable for establishing proper cell polarity (Ori-McKenney et al., 2012; Zhu and Kaverina, 2013). Further studies should therefore address whether Chc organizes oocyte MT polarity by nucleating MT at the TGN.

Model for *Bic-D* and *Chc* functions in establishing pole plasm and anterior-posterior (A-P) axis

Incorporating our results into a model, we show how endocytosis, pole plasm assembly and anchoring of the pole plasm are tightly linked processes involving feedback loop regulation (Fig. 9). *Bic-D* contributes to *osk* mRNA localization and pole plasm assembly in two ways. First, from earlier studies we learned that the dynein adaptor Bic-D acts directly by transporting *osk* mRNA from the nurse cells into the oocyte (Suter and Steward, 1991; Swan and Suter, 1996; Clark et al., 2007). Here, we found that *Bic-D* controls the endocytic pathway also by transporting *Chc* mRNA into the oocyte and by localizing Chc protein to the oocyte cortex and enriching it at the posterior cortex. *Bic-D* is additionally involved in polarizing the endocytic pathway by directly or indirectly (e.g. through localization of Chc or *osk* mRNA/Osk protein) localizing the endocytic proteins Rab11 and Rbsn-5. Thus, through these mechanisms, *Bic-D* promotes endocytosis at the posterior, which then stimulates pole plasm anchoring and *osk* mRNA

Development (2014) 141, 1915-1926 doi:10.1242/dev.099432

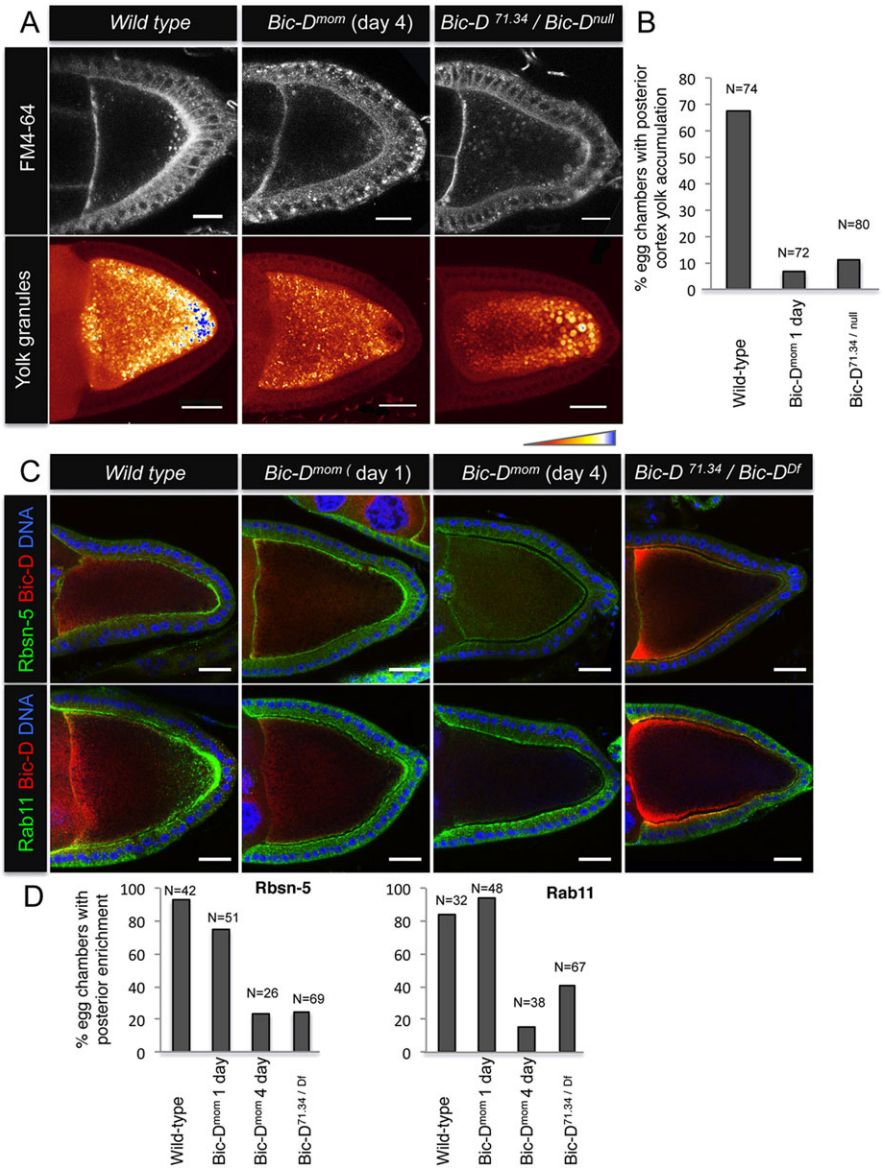

Fig. 8. *Bic-D* is required for correct posterior endocytosis. (A,B) Endocytosis activity was analyzed using the FM4-64 uptake assay and by imaging autofluorescence of yolk granules in wild-type, *Bic-D*^{mom} (4 days after turning off *Bic-D* expression) and *Bic-D*$^{71.34}$/*Bic-D*^{null} egg chambers. Posterior endocytosis and polarized distribution are only distinctly seen in the wild type. (C,D) Antibody staining of *Bic-D*$^{71.34}$/*Bic-D*^{Df}, *Bic-D*^{mom} (4 days) and *Bic-D*^{mom} egg chambers still containing Bic-D (1 day after turning off *Bic-D* expression) show that posterior enrichment of Rbsn-5 and Rab11 at the oocyte cortex correlates with the presence of wild-type Bic-D protein. Scale bars: 20 µm (A, upper panels; C); 30 µm (A, lower panels).

localization at the posterior. *Chc* is also needed for establishing the MT cytoskeleton during the middle stages of oogenesis and it may be needed for the maintenance of this A-P polarity. In summary, we have found a novel and central role for Chc and Bic-D proteins in controlling pole plasm assembly by affecting MT polarity, endocytosis and *osk* mRNA localization.

MATERIALS AND METHODS

Drosophila stocks

Gal4 lines, *Chc*^{4} and *Chc*^{1} stocks were obtained from the Bloomington *Drosophila* Stock Center. The transgenic genomic rescue constructs *pCHC3w*$^{+}$ and *4C-CHC* [FLAG-Tetracysteine tag (4C)] were from C. Bazinet and P. Verstreken (Bazinet et al., 1993; Kasprowicz et al., 2008), and *UAS-Chc::eGFP. Tub-Egl::eGFP* flies were from S. Bullock (Dienstbier et al., 2009; Li et al., 2010). *Bic-D*$^{71.34}$ and *Bic-D*^{IIIE48}, the two dominant alleles, the null allele *Bic-D*^{r5} and *Bic-D*^{mom} were described previously (Suter et al., 1989; Ran et al., 1994; Swan and Suter, 1996) except that *Df(2L)Exel7068* (Exelixis) was used as *Bic-D*-deficiency. *Chc*^{GF23} (from T. Schüpbach) (Yan et al., 2009), *Rab5*^{2} (Lu and Bilder, 2005) and *Rbsn-5*^{C241} (from A. Nakamura) (Tanaka and Nakamura, 2008) were used to generate mutant germ line clones with *hsFLP; Ubi-GFP (S65T)nls FRT40A*, His2Av-GFP, hsFLP, FRT19A/FM7a or Ubi-GFP, hsFLP, FRT19A/FM7. Clones were induced twice per day at 37°C for 2 h for 2 consecutive days. Flies were dissected 2-4 days after hatching. The *Chc*^{4} chromosome from the Bloomington *Drosophila* Stock Center was cleaned up by recombination with the multiply marked X chromosome *c v m w y sd os*, resulting in a lethal-free *Chc*^{4} chromosome marked with *sd*. Production of homozygous *Chc*^{4} females was described previously (Bazinet et al., 1993). *pUASP-Chc-V5-K10-attB* and *pUASP-myc-chc-K10-attB* transgenic flies were generated with the phiC31 integrase transgenesis system and the *y w*;+; *attP-64A* line as host (Bischof et al., 2007; Koch et al., 2009).

To express *UAS-Chc::eGFP* in the *Bic-D*^{mom} mutant background, the *P{matα4-GAL-VP16}* driver was recombined with the *Bic-D* deficiency *Df(2L)Exel7068*. Flies of the genotype *Df(2L)Exel7068, P{matα4-GAL-VP16}/SM1; hs-BicD/TM3Sb* were crossed to *BicD*^{r5}*/SM1; UAS-Chc::eGFP/TM3Sb* flies and the progeny of this cross was heat shocked twice per day (37°C, 2 h) from L3 till at least day two of adulthood, before shutting off *Bic-D* expression. Otherwise, flies were kept at 25°C.

DNA constructs

To construct *pUASP-myc-Chc-K10-attB* and *pUASP-Chc-V5-K10-attB*, the *Chc* open reading frame was amplified from LD43101 (BDGP) using primers with *Xba*I sites for cloning in-frame into *pUASP-myc-K10-attB* and *pMT-V5-HisA* (Life Technologies), respectively. From the

Development (2014) 141, 1915-1926 doi:10.1242/dev.099432

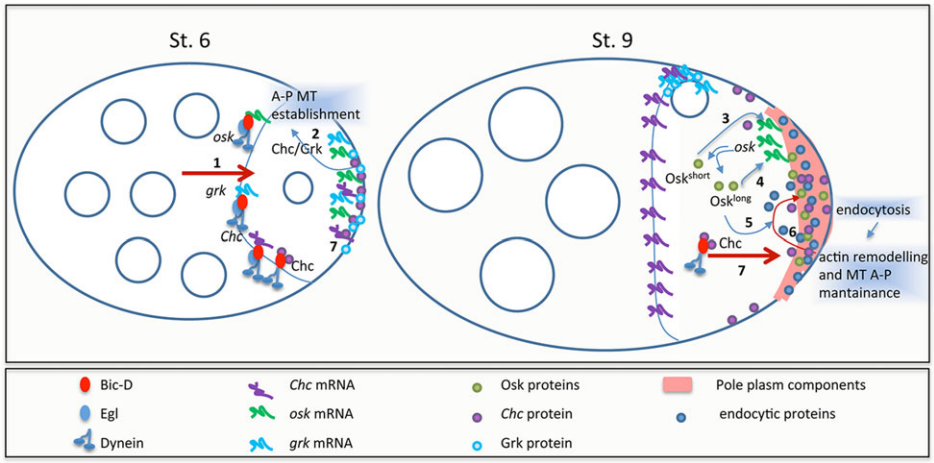

Fig. 9. Model of the involvement of Bic-D and Chc in establishing oocyte polarity. Bic-D contributes to pole plasm assembly in two ways. First, Bic-D transports *osk* and *grk* mRNAs from the nurse cells into the oocyte (1) (Suter and Steward, 1991; Swan and Suter, 1996; Clark et al., 2007). Grk signaling to the posterior follicle cells during stages 6-7 initiates reorganization of the MTs within the oocyte (2). This MT organization directs *osk* RNA to the posterior where it is translated from stage 9 onwards into two Osk isoforms, which initiate assembly of the pole plasm. Short Osk recruits downstream pole plasm components to the posterior (3), and long Osk maintains *osk* mRNA localization (4) (Markussen et al., 1995; Breitwieser et al., 1996; Vanzo and Ephrussi, 2002). Long Osk also stimulates endocytosis at the posterior cortex in part by recruiting endocytic proteins (5) (Vanzo et al., 2007; Tanaka and Nakamura, 2008). This endocytosis triggers the formation of long F actin projections that help to anchor pole plasm components, thereby forming the known feedback loop (6) (Vanzo et al., 2007; Tanaka and Nakamura, 2008). Because pole plasm anchoring seems to increase posterior localization of *osk* RNA, long Osk-induced endocytosis and actin remodeling have been suggested to form another feedback loop (Tanaka and Nakamura, 2011). However, a more direct role of endocytosis in *osk* mRNA localization cannot be dismissed. Second, *Bic-D* controls the endocytic pathway also by transporting *Chc* mRNA and Chc protein into the oocyte during early oogenesis (1) and by transporting Chc protein to the oocyte cortex and enriching it at the posterior cortex (7). Chc is also needed for A-P MT establishment during the middle stages of oogenesis (2) and possibly for the maintenance of this polarity.

resulting *pMT-Chc-V5* template, the *Chc-V5* region was amplified with primers containing *Not*I and *Kpn*I sites to facilitate cloning into the *pUASP-K10-attB* vector.

Immunoprecipitations and western blots

Immunoprecipitations (IPs) were performed according to Vazquez-Pianzola et al. (Vazquez-Pianzola et al., 2011) with embryonic extracts from 0- to 8-hour-old *translin*^{null} mutant embryos and from same age embryos laid by *Nullo-Gal4/SM1*; *pUASP-myc-Chc-K10 attB/TM3Sb* females. For IPs, 70 pairs of ovaries were used per ovarian IP, whereas seven pairs were collected for one western blot lane. These were boiled for 2 min in 20 µl of SDS sample buffer, vortexed for 15 s, boiled for another 8 min and loaded on a SDS-PAGE gel. Western blots were performed using the mouse monoclonal anti-myc 9E10 [1:5, Developmental Studies Hybridoma Bank (DSHB)], anti-Egl (1:5000) (Mach and Lehmann, 1997), mouse anti-Bic-D antibodies (1B11 plus 4C2, 1:10) (Suter and Steward, 1991), mouse anti-α-Tubulin AA4.3 (1:2000, DSHB), rabbit anti-mammalian Chc (1:500) (Hirst et al., 2009) and rabbit anti-Flag (1:320; Sigma, F7425). Horseradish peroxidase-conjugated secondary antibodies were from GE Healthcare (NA934V and NA931V).

Immunostaining

Whole-mount immunostainings were performed with mouse anti-Bic-D (1B11 plus 4C2, 1:10) (Suter and Steward, 1991), rat anti-Chc (1:35) (Wingen et al., 2009) or rabbit anti-Chc (1:200) (Kametaka et al., 2010), rabbit anti-Osk (1:500) (Markussen et al., 1995), rabbit anti-Egl (1:5000) (Mach and Lehmann, 1997), rabbit anti-Staufen (1:2000) (St Johnston et al., 1991), mouse anti-myc 9E10 (1:5, DSHB), mouse anti-Flag (1:200, Sigma, F3165), rabbit anti-Flag (1:200, Sigma, F7425), rabbit anti-Rab11 (1:8000) (Tanaka and Nakamura, 2008), rabbit anti-Rbsn-5 (1:5000) (Tanaka and Nakamura, 2008), rabbit anti-Khc (1:150, Cytoskeleton), mouse anti-α-tubulin DM1A (1:500, Sigma, T9026), rabbit anti-EB1 (1:500) (Rogers et al., 2002) and rabbit anti-Clc (1:500) (Heerssen et al., 2008). Both anti-Flag antibodies stained the oocyte nucleus in wild-type ovaries. To reduce this background cross-reactivity, antibodies were preadsorbed on wild-type embryos. Secondary antibodies were Cy3-conjugated anti-mouse (712-165-150), Cy5-conjugated anti-rabbit (111-175-144), Cy5-conjugated anti-mouse (115-175-146) (Jackson ImmunoResearch) and A488-conjugated goat anti-rabbit (A11008, Molecular Probes). Nuclei and F-actin were stained for 20 min with 2.5 µg/ml Hoechst 33258 and 1 unit/ml rhodamine-conjugated phalloidin (Molecular Probes), respectively, during the final washing steps. Imaging was with a Leica TCS-SP2 confocal microscope. Mouse anti-α-tubulin DM1A staining of ovaries is described by Sato et al. (Sato et al., 2011) and EB1 staining by Sanghavi et al. (Sanghavi et al., 2012).

In situ hybridization to whole-mount ovaries

Digoxigenin-labeled RNA probes were synthesized from linearized pBS-*oskar*, ESTs LD32255 and LD43101 (BDGP), pBS-*OrbE4* cDNA (Lantz et al., 1992) and pBS-*Bic-D*. *In situ* hybridizations experiments (Vazquez-Pianzola et al., 2011) utilized 5% milk for blocking and as antibody dilution buffer. For dual detection of mRNA and GFP signal, the proteinase K step was omitted. Rabbit anti-GFP (1:300, AMS Biotechnology, 210-PS-1GFP) was incubated overnight together with sheep anti-digoxigenin antibodies (Roche, 1 333 089). Donkey anti-sheep A647 (1:200, Jackson ImmunoResearch, 713-606-147) and donkey anti-rabbit A568 (1:1500, Invitrogen, A10042) secondary antibodies were incubated overnight.

RT-qPCR assays and RNA immunoprecipitation

RNA from five to ten ovaries was extracted using the RNeasy Kit (Qiagen), DNaseI digestion was performed according to the manual. RNA IPs were performed essentially as described (Easow et al., 2007) with the following modifications. Blocking buffer was supplemented with 1 mg/ml bovine serum albumin and protease inhibitors (Roche). The following were added to the hypotonic buffer: 1 mM DTT, 0.5% Tween-20, protease and RNase inhibitors, 100 U/ml (Biolabs). The wash buffer contained 200 mM KCl. For each IP, 40 µl of protein G sepharose beads (Roche) and 1 ml of monoclonal anti-GFP were used (a gift from A. Marcil). Coated beads were washed with non-hypotonic buffer (hypotonic buffer adjusted to 150 mM KCl and 20% glycerol). For extract preparation, 1 g of 0- to 8-hour-old embryos were homogenized in 1 ml hypotonic buffer. The extract was cleared at 10,000× ***g*** for 20 min. For each IP, 600 µl of cleared supernatant was adjusted to 20% glycerol and 150 mM KCl, and supplemented with 2 µl of RNase-free DNase

I (20 U/ml, Roche). IP was performed overnight. The immunoprecipitate was washed eight times. Beads were Proteinase K treated, RNA extracted using Trizol (Invitrogen) and resuspended in 25 µl DEPC-treated water, ready for RT-qPCR analysis.

cDNAs were synthesized with the SuperScript II Reverse Transcriptase and oligo dT primers. Primers used for the RT-qPCR analysis amplified fragments between 100 and 150 bp and one primer of a pair spanned an exon junction. The QuantiTect SYBR Green PCR Kit (Qiagen) and a Rotor Gene (Qiagen) were used, and the Pfaffl method was applied to normalize to Tubulin67C mRNA levels and to calculate fold changes (Pfaffl, 2001).

Endocytosis assay and live imaging

For FM4-64 (Molecular Probes) incorporation assays, see Sommer et al. (Sommer et al., 2005). For live imaging of egg chambers, five to seven females were raised with five to seven males on freshly prepared fly food supplemented with fresh yeast paste. For *BicD*^{mom} mutants, fly food was changed every day for 5 days. Ovaries were extracted into modified Schneider's medium (Prasad et al., 2007) and transferred into a drop of 10S Voltalef oil. Ovarioles were stretched by dragging their anterior end from the medium into the oil, immobilizing the ovarioles at the medium-oil interface. Pictures were acquired on a Till Photonics iMIC spinning disc (60× lens, Andor 897 EMCCD) every 500 ms for 200 cycles. Linearly moving particles were selected by hand and particle velocity was calculated using ImageJ.

Acknowledgements

We thank S. Bullock, C. Bazinet, P. Verstreken, P. Behr, A. M. Nakamura, R. Lehmann., J. Hirst, S. Robinson, S. Waguri, S. L. Rogers, A. Marcil, D. St Johnston, T. Schüpbach, D. Bilder and D. Graeme for antibodies, constructs and fly stocks. We also thank G. Hernandez and S. Bullock for providing most constructive input for this manuscript. Special thanks go to D. Beuchle and B. Schaller for their excellent technical help.

Competing interests

The authors declare no competing financial interests.

Author contributions

P.V.-P., J.A., D. Haldemann, D. Hain and H.U. performed experiments and data analysis. P.V.-P. and B.S. conceived the studies, performed data analysis and wrote the manuscript.

Funding

This work was supported by a grant from the Swiss National Science Foundation, by the Canton of Bern and by a grant from the Mittelbauvereinigung der Universität Bern (MVUB) to P.V.-P.

Supplementary material

Supplementary material available online at
http://dev.biologists.org/lookup/suppl/doi:10.1242/dev.099432/-/DC1

References

Bazinet, C., Katzen, A. L., Morgan, M., Mahowald, A. P. and Lemmon, S. K. (1993). The Drosophila clathrin heavy chain gene: clathrin function is essential in a multicellular organism. *Genetics* **134**, 1119-1134.

Bianco, A., Dienstbier, M., Salter, H. K., Gatto, G. and Bullock, S. L. (2010). Bicaudal-D regulates fragile X mental retardation protein levels, motility, and function during neuronal morphogenesis. *Curr. Biol.* **20**, 1487-1492.

Bischof, J., Maeda, R. K., Hediger, M., Karch, F. and Basler, K. (2007). An optimized transgenesis system for Drosophila using germ-line-specific phiC31 integrases. *Proc. Natl. Acad. Sci. U.S.A.* **104**, 3312-3317.

Booth, D. G., Hood, F. E., Prior, I. A. and Royle, S. J. (2011). A TACC3/ch-TOG/clathrin complex stabilises kinetochore fibres by inter-microtubule bridging. *EMBO J.* **30**, 906-919.

Breitwieser, W., Markussen, F. H., Horstmann, H. and Ephrussi, A. (1996). Oskar protein interaction with Vasa represents an essential step in polar granule assembly. *Genes Dev.* **10**, 2179-2188.

Brodsky, F. M. (2012). Diversity of clathrin function: new tricks for an old protein. *Annu. Rev. Cell Dev. Biol.* **28**, 309-336.

Bullock, S. L. and Ish-Horowicz, D. (2001). Conserved signals and machinery for RNA transport in Drosophila oogenesis and embryogenesis. *Nature* **414**, 611-616.

Clark, A., Meignin, C. and Davis, I. (2007). A Dynein-dependent shortcut rapidly delivers axis determination transcripts into the Drosophila oocyte. *Development* **134**, 1955-1965.

Claussen, M. and Suter, B. (2005). BicD-dependent localization processes: from Drosophilia development to human cell biology. *Ann. Anat.* **187**, 539-553.

Dienstbier, M., Boehl, F., Li, X. and Bullock, S. L. (2009). Egalitarian is a selective RNA-binding protein linking mRNA localization signals to the dynein motor. *Genes Dev.* **23**, 1546-1558.

Dollar, G., Struckhoff, E., Michaud, J. and Cohen, R. S. (2002). Rab11 polarization of the Drosophila oocyte: a novel link between membrane trafficking, microtubule organization, and oskar mRNA localization and translation. *Development* **129**, 517-526.

Easow, G., Teleman, A. A. and Cohen, S. M. (2007). Isolation of microRNA targets by miRNP immunopurification. *RNA* **13**, 1198-1204.

Ephrussi, A., Dickinson, L. K. and Lehmann, R. (1991). Oskar organizes the germ plasm and directs localization of the posterior determinant nanos. *Cell* **66**, 37-50.

Faini, M., Beck, R., Wieland, F. T. and Briggs, J. A. G. (2013). Vesicle coats: structure, function, and general principles of assembly. *Trends Cell Biol.* **23**, 279-288.

Fridolfsson, H. N., Ly, N., Meyerzon, M. and Starr, D. A. (2010). UNC-83 coordinates kinesin-1 and dynein activities at the nuclear envelope during nuclear migration. *Dev. Biol.* **338**, 237-250.

Heerssen, H., Fetter, R. D. and Davis, G. W. (2008). Clathrin dependence of synaptic-vesicle formation at the Drosophila neuromuscular junction. *Curr. Biol.* **18**, 401-409.

Hirst, J., Sahlender, D. A., Choma, M., Sinka, R., Harbour, M. E., Parkinson, M. and Robinson, M. S. (2009). Spatial and functional relationship of GGAs and AP-1 in Drosophila and HeLa cells. *Traffic* **10**, 1696-1710.

Hughes, J. R., Bullock, S. L. and Ish-Horowicz, D. (2004). Inscuteable mRNA localization is dynein-dependent and regulates apicobasal polarity and spindle length in Drosophila neuroblasts. *Curr. Biol.* **14**, 1950-1956.

Jankovics, F., Sinka, R. and Erdelyi, M. (2001). An interaction type of genetic screen reveals a role of the Rab11 gene in oskar mRNA localization in the developing Drosophila melanogaster oocyte. *Genetics* **158**, 1177-1188.

Januschke, J., Nicolas, E., Compagnon, J., Formstecher, E., Goud, B. and Guichet, A. (2007). Rab6 and the secretory pathway affect oocyte polarity in Drosophila. *Development* **134**, 3419-3425.

Kametaka, S., Sawada, N., Bonifacino, J. S. and Waguri, S. (2010). Functional characterization of protein-sorting machineries at the trans-Golgi network in Drosophila melanogaster. *J. Cell Sci.* **123**, 460-471.

Kasprowicz, J., Kuenen, S., Miskiewicz, K., Habets, R. L. P., Smitz, L. and Verstreken, P. (2008). Inactivation of clathrin heavy chain inhibits synaptic recycling but allows bulk membrane uptake. *J. Cell Biol.* **182**, 1007-1016.

Kim-Ha, J., Smith, J. L. and Macdonald, P. M. (1991). oskar mRNA is localized to the posterior pole of the Drosophila oocyte. *Cell* **66**, 23-35.

Koch, R., Ledermann, R., Urwyler, O., Heller, M. and Suter, B. (2009). Systematic functional analysis of Bicaudal-D serine phosphorylation and intragenic suppression of a female sterile allele of BicD. *PLoS ONE* **4**, e4552.

Lantz, V., Ambrosio, L. and Schedl, P. (1992). The Drosophila orb gene is predicted to encode sex-specific germline RNA-binding proteins and has localized transcripts in ovaries and early embryos. *Development* **115**, 75-88.

Larsen, K. S., Xu, J., Cermelli, S., Shu, Z. and Gross, S. P. (2008). BicaudalD actively regulates microtubule motor activity in lipid droplet transport. *PLoS ONE* **3**, e3763.

Li, X., Kuromi, H., Briggs, L., Green, D. B., Rocha, J. J., Sweeney, S. T. and Bullock, S. L. (2010). Bicaudal-D binds clathrin heavy chain to promote its transport and augments synaptic vesicle recycling. *EMBO J.* **29**, 992-1006.

Lu, H. and Bilder, D. (2005). Endocytic control of epithelial polarity and proliferation in Drosophila. *Nat. Cell Biol.* **7**, 1232-1239.

Mach, J. M. and Lehmann, R. (1997). An Egalitarian-BicaudalD complex is essential for oocyte specification and axis determination in Drosophila. *Genes Dev.* **11**, 423-435.

Markussen, F. H., Michon, A. M., Breitwieser, W. and Ephrussi, A. (1995). Translational control of oskar generates short OSK, the isoform that induces pole plasma assembly. *Development* **121**, 3723-3732.

Matanis, T., Akhmanova, A., Wulf, P., Del Nery, E., Weide, T., Stepanova, T., Galjart, N., Grosveld, F., Goud, B., De Zeeuw, C. I. et al. (2002). Bicaudal-D regulates COPI-independent Golgi-ER transport by recruiting the dynein-dynactin motor complex. *Nat. Cell Biol.* **4**, 986-992.

Moon, W. and Hazelrigg, T. (2004). The Drosophila microtubule-associated protein mini spindles is required for cytoplasmic microtubules in oogenesis. *Curr. Biol.* **14**, 1957-1961.

Morrison, H. A., Dionne, H., Rusten, T. E., Brech, A., Fisher, W. W., Pfeiffer, B. D., Celniker, S. E., Stenmark, H. and Bilder, D. (2008). Regulation of early endosomal entry by the Drosophila tumor suppressors Rabenosyn and Vps45. *Mol. Biol. Cell* **19**, 4167-4176.

Navarro, C., Puthalakath, H., Adams, J. M., Strasser, A. and Lehmann, R. (2004). Egalitarian binds dynein light chain to establish oocyte polarity and maintain oocyte fate. *Nat. Cell Biol.* **6**, 427-435.

Ori-McKenney, K. M., Jan, L. Y. and Jan, Y.-N. (2012). Golgi outposts shape dendrite morphology by functioning as sites of acentrosomal microtubule nucleation in neurons. *Neuron* **76**, 921-930.

Peralta, S., Gómez, Y., González-Gaitán, M. A., Moya, F. and Vinós, J. (2009). Notch down-regulation by endocytosis is essential for pigment cell determination and survival in the Drosophila retina. *Mech. Dev.* **126**, 256-269.
Pfaffl, M. W. (2001). A new mathematical model for relative quantification in real-time RT-PCR. *Nucleic Acids Res.* **29**, e45.
Prasad, M., Jang, A. C., Starz-Gaiano, M., Melani, M. and Montell, D. J. (2007). A protocol for culturing *Drosophila melanogaster* stage 9 egg chambers for live imaging. *Nat. Protoc.* **2**, 2467-2473.
Ran, B., Bopp, R. and Suter, B. (1994). Null alleles reveal novel requirements for Bic-D during Drosophila oogenesis and zygotic development. *Development* **120**, 1233-1242.
Rogers, S. L., Rogers, G. C., Sharp, D. J. and Vale, R. D. (2002). Drosophila EB1 is important for proper assembly, dynamics, and positioning of the mitotic spindle. *J. Cell Biol.* **158**, 873-884.
Royle, S. J., Bright, N. A. and Lagnado, L. (2005). Clathrin is required for the function of the mitotic spindle. *Nature* **434**, 1152-1157.
Sanghavi, P., Lu, S. and Gonsalvez, G. B. (2012). A functional link between localized Oskar, dynamic microtubules, and endocytosis. *Dev. Biol.* **367**, 66-77.
Sato, K., Nishida, K. M., Shibuya, A., Siomi, M. C. and Siomi, H. (2011). Maelstrom coordinates microtubule organization during Drosophila oogenesis through interaction with components of the MTOC. *Genes Dev.* **25**, 2361-2373.
Sommer, B., Oprins, A., Rabouille, C. and Munro, S. (2005). The exocyst component Sec5 is present on endocytic vesicles in the oocyte of Drosophila melanogaster. *J. Cell Biol.* **169**, 953-963.
Splinter, D., Tanenbaum, M. E., Lindqvist, A., Jaarsma, D., Flotho, A., Yu, K. L., Grigoriev, I., Engelsma, D., Haasdijk, E. D., Keijzer, N. et al. (2010). Bicaudal D2, dynein, and kinesin-1 associate with nuclear pore complexes and regulate centrosome and nuclear positioning during mitotic entry. *PLoS Biol.* **8**, e1000350.
St Johnston, D., Beuchle, D. and Nüsslein-Volhard, C. (1991). Staufen, a gene required to localize maternal RNAs in the Drosophila egg. *Cell* **66**, 51-63.
Suter, B. and Steward, R. (1991). Requirement for phosphorylation and localization of the Bicaudal-D protein in Drosophila oocyte differentiation. *Cell* **67**, 917-926.
Suter, B., Romberg, L. M. and Steward, R. (1989). Bicaudal-D, a Drosophila gene involved in developmental asymmetry: localized transcript accumulation in ovaries and sequence similarity to myosin heavy chain tail domains. *Genes Dev.* **3**, 1957-1968.
Swan, A. and Suter, B. (1996). Role of Bicaudal-D in patterning the Drosophila egg chamber in mid-oogenesis. *Development* **122**, 3577-3586.
Swan, A., Nguyen, T. and Suter, B. (1999). Drosophila Lissencephaly-1 functions with Bic-D and dynein in oocyte determination and nuclear positioning. *Nat. Cell Biol.* **1**, 444-449.
Tanaka, T. and Nakamura, A. (2008). The endocytic pathway acts downstream of Oskar in Drosophila germ plasm assembly. *Development* **135**, 1107-1117.
Tanaka, T. and Nakamura, A. (2011). Oskar-induced endocytic activation and actin remodeling for anchorage of the Drosophila germ plasm. *Bioarchitecture* **1**, 122-126.
Tanaka, T., Kato, Y., Matsuda, K., Hanyu-Nakamura, K. and Nakamura, A. (2011). Drosophila Mon2 couples Oskar-induced endocytosis with actin remodeling for cortical anchorage of the germ plasm. *Development* **138**, 2523-2532.
Vanzo, N. F. and Ephrussi, A. (2002). Oskar anchoring restricts pole plasm formation to the posterior of the Drosophila oocyte. *Development* **129**, 3705-3714.
Vanzo, N., Oprins, A., Xanthakis, D., Ephrussi, A. and Rabouille, C. (2007). Stimulation of endocytosis and actin dynamics by Oskar polarizes the Drosophila oocyte. *Dev. Cell* **12**, 543-555.
Vazquez-Pianzola, P. and Suter, B. (2012). Conservation of the RNA Transport Machineries and Their Coupling to Translation Control across Eukaryotes. *Comp. Funct. Genomics* **2012**, 1-13.
Vazquez-Pianzola, P., Urlaub, H. and Suter, B. (2011). Pabp binds to the osk 3'UTR and specifically contributes to osk mRNA stability and oocyte accumulation. *Dev. Biol.* **357**, 404-418.
Wanschers, B. F. J., van de Vorstenbosch, R., Schlager, M. A., Splinter, D., Akhmanova, A., Hoogenraad, C. C., Wieringa, B. and Fransen, J. A. M. (2007). A role for the Rab6B Bicaudal-D1 interaction in retrograde transport in neuronal cells. *Exp. Cell. Res.* **313**, 3408-3420.
Wingen, C., Stümpges, B., Hoch, M. and Behr, M. (2009). Expression and localization of clathrin heavy chain in Drosophila melanogaster. *Gene Expr. Patterns* **9**, 549-554.
Yan, Y., Denef, N. and Schüpbach, T. (2009). The vacuolar proton pump, V-ATPase, is required for notch signaling and endosomal trafficking in Drosophila. *Dev. Cell* **17**, 387-402.
Zhu, X. and Kaverina, I. (2013). Golgi as an MTOC: making microtubules for its own good. *Histochem. Cell Biol.* **140**, 361-367.

Supplementary Material S1:

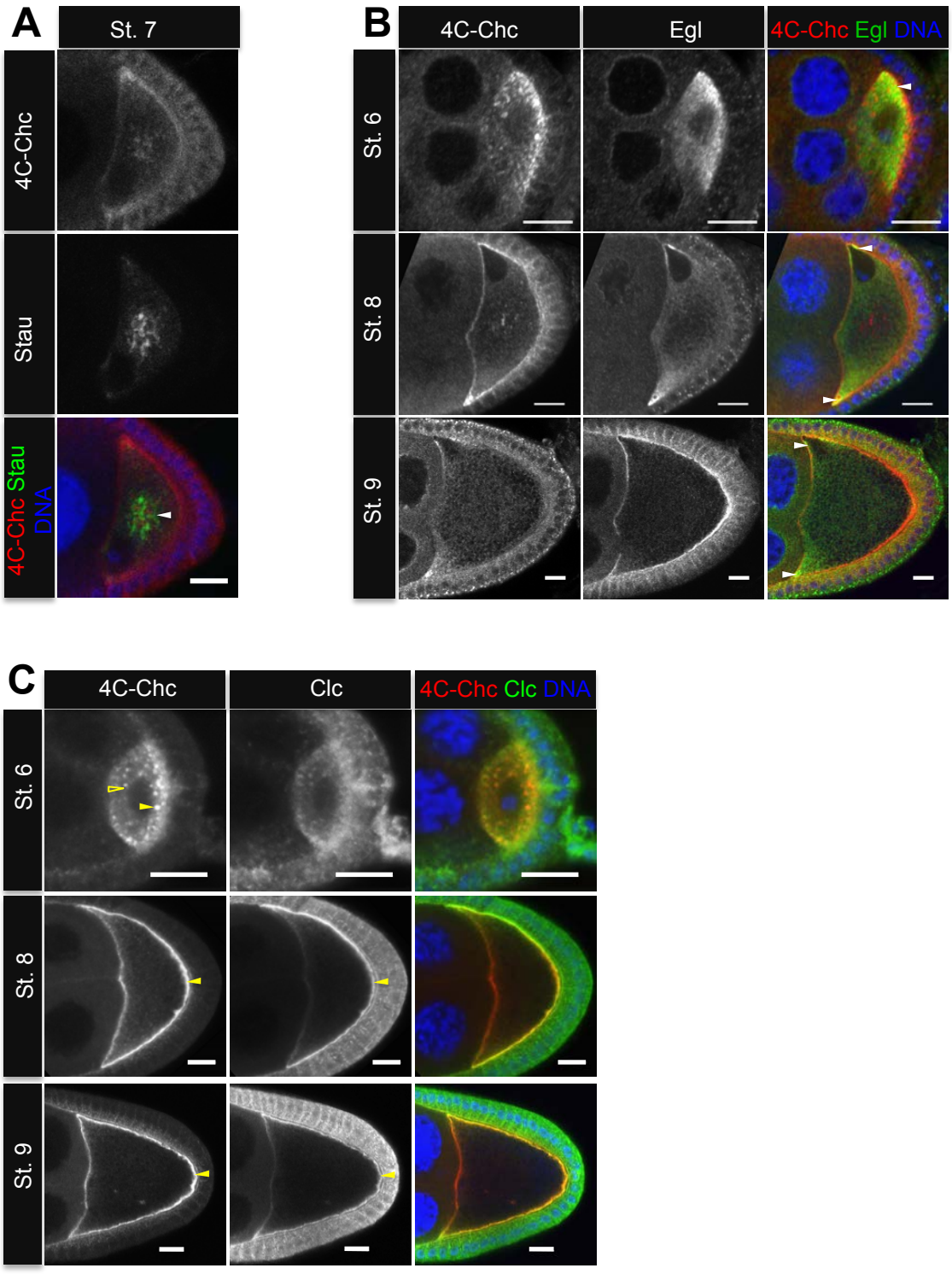

Legend for Supplementary Material S1:
(A) Immunostaining of 4C-CHC expressing ovarioles with anti-Flag (to detect Flag::Chc) and anti-Staufen antibodies. In stage 7-8, a Chc enrichment was detected in the center of the oocyte (see also Figure 1E, H). This was seen when probing for endogenous Chc, UAS-Chc::GFP and 4C-Chc, but it was not seen with Myc::Chc and Chc::V5 staining (see Figure 1E, H; data not shown). We have not tested whether the differences are due to differences in expression levels. Interestingly, this localization pattern resembles the one of Stau and several endosomal proteins (Tanaka and Nakamura, 2008). Stau and Chc are both enriched in the center of the oocyte by stage 6-8. However, the two do not completely co-localize in this central structure. **(B)** Immunostaining of 4C-CHC expressing ovarioles with anti-Flag and anti-Egl antibodies. In stage 6 oocytes Chc shows a partial co-localization with Bic-D and Egl at the posterior cortex (arrowhead) (see also Figure 1H). A second partial co-localization between Bic-D / Egl and Chc is evident at the anterior cortex in stage 8 egg chambers (arrowhead, see also Figure 1H). However, in stage 7-8 egg chambers Bic-D and Egl are excluded from the central region where Chc additionally accumulates (see also Figure 1H). **(C)** Immunostaining of 4C-CHC expressing ovarioles with anti-Flag (to detect Chc) and anti-Clc antibodies. In stage 6 Clc and Chc accumulate in the oocyte and both show an enrichment towards the posterior cortex. However co-localization is not complete. Particles showing strong Chc and Clc staining (open arrowhead), but also others showing only strong Chc enrichment (arrowhead) are observed. Colocalization at the oocyte cortex is also observed in st. 8-9 oocytes. However, while Chc shows an enrichment at the posterior cortex, Clc shows a more uniform cortical accumulation (arrowheads in stage 8 and 9). Endogenous Clc is also strongly expressed in the somatic follicle cells around the oocyte. Scale bars: 10 μm.

Supplementary Material S2:

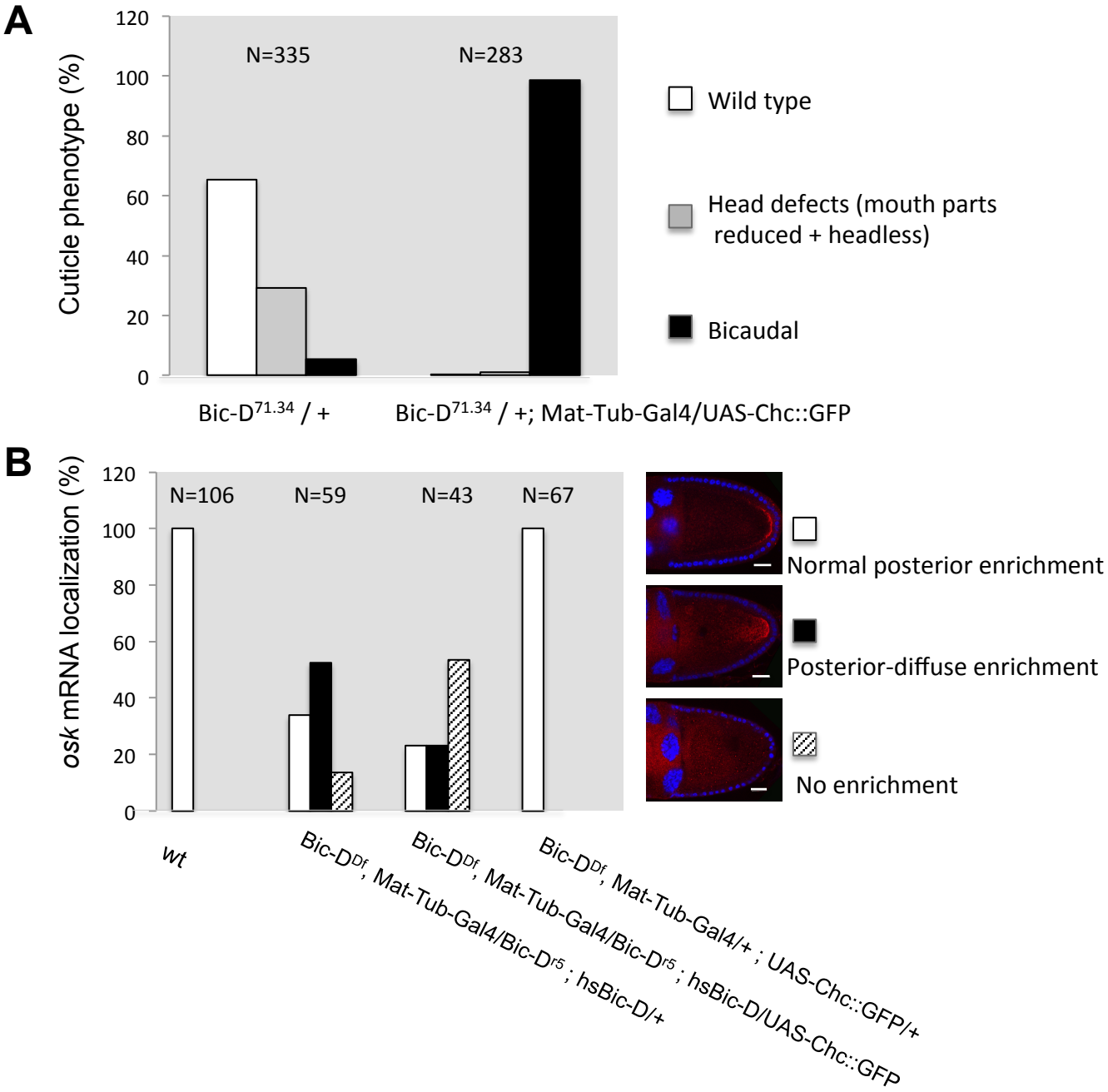

Legend for Supplementary Material S2:

Genetic interaction between *Bic-D* and *Chc*. Overexpression of *Chc::GFP* enhances the *osk* mislocalization phenotypes in *Bic-D* dominant and in *Bic-D*^{null} backgrounds.
(A) Cuticles were prepared from embryos laid by mothers of the depicted genotypes, and embryonic phenotypes were scored as indicated. Overexpression of the Chc::GFP fusion protein enhanced the bicaudal phenotype of the *Bic-D*$^{71.34}$ dominant allele**.** A possible reason for this could be that the overexpression leads to slightly enhanced endocytosis and thereby to enhanced cortical anchoring of ectopic *osk* mRNA.
(B) *In situ* hybridization to ovaries of the indicated genotypes using digoxigenin-labeled antisense RNA probes against *osk* mRNA. Localization of *osk* mRNA in stage 9-10 egg chambers was scored as depicted. *osk* mRNA signal is in red, DNA staining in blue. In *wild-type* oocytes *osk* signal is strong and focused at the posterior pole (white bars). In *Bic-D*^{mom} oocytes *osk* signal was overall weaker and many egg chambers showed more diffuse posterior signals or uniform/no signal (black and dashed bars). The mutant phenotype was enhanced by overexpressing Chc::GFP. This was not due to overexpression of Chc::GFP by itself, since overexpression in egg chambers containing one functional *Bic-D* copy did not alter *osk* mRNA localization (4th genotype). Competition for Bic-D by the two different cargoes *osk* mRNA/Egl and Chc protein could account for the reduced posterior localization of *osk* mRNA. Scale bars: 20µm.

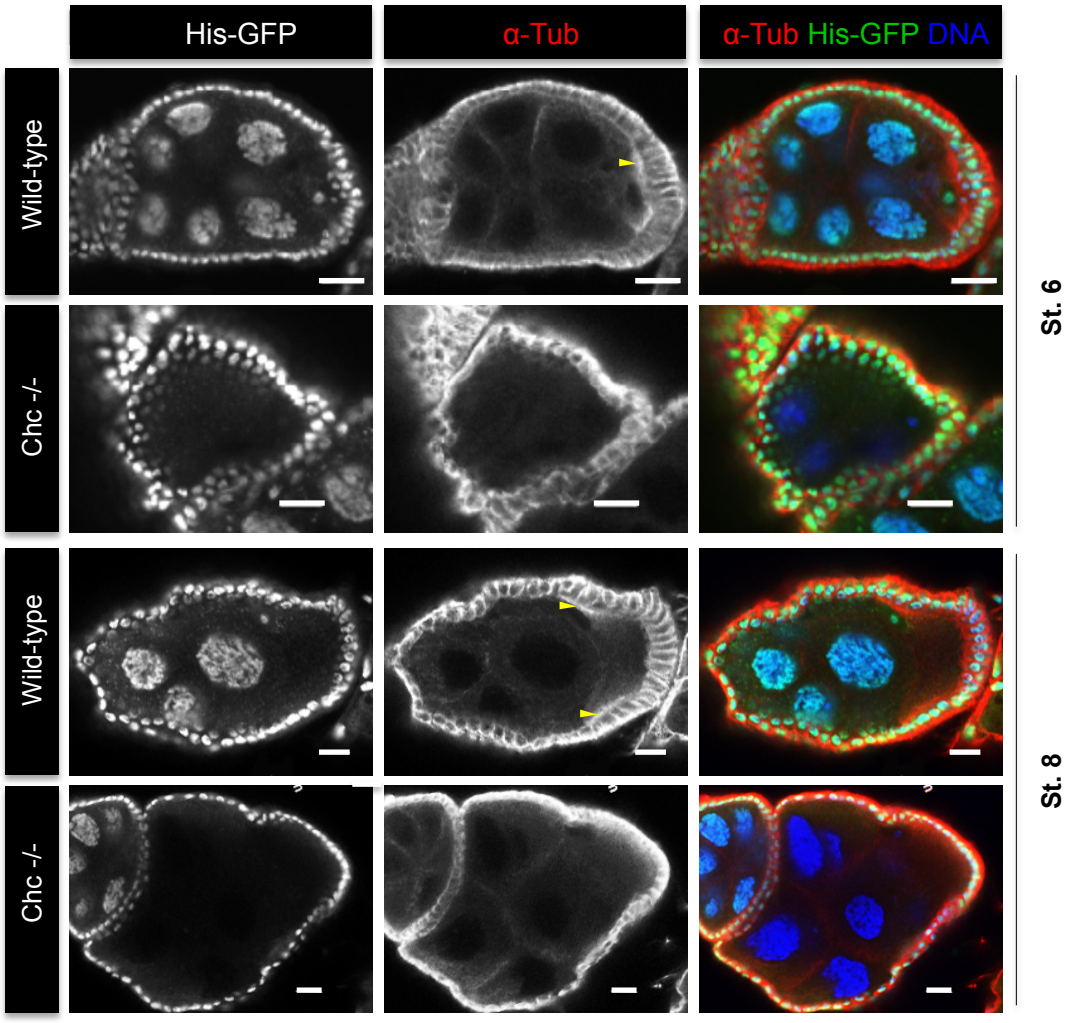

Supplementary Material S3:

Oocyte microtubule polarity is affected in *Chc*^{null} germline clones. Germline clones for a null allele of *Chc*, *Chc*^{GF23} were generated and stained with anti-alpha tubulin antibodies (red). Mutant clones are marked by the absence of His-GFP. Focusing of microtubules (arrowheads) stained with alpha-tubulin is affected in mutant egg chambers. Ovarioles were also stained with Hoechst (blue) to visualize the DNA. Scale bars: 10 µm.

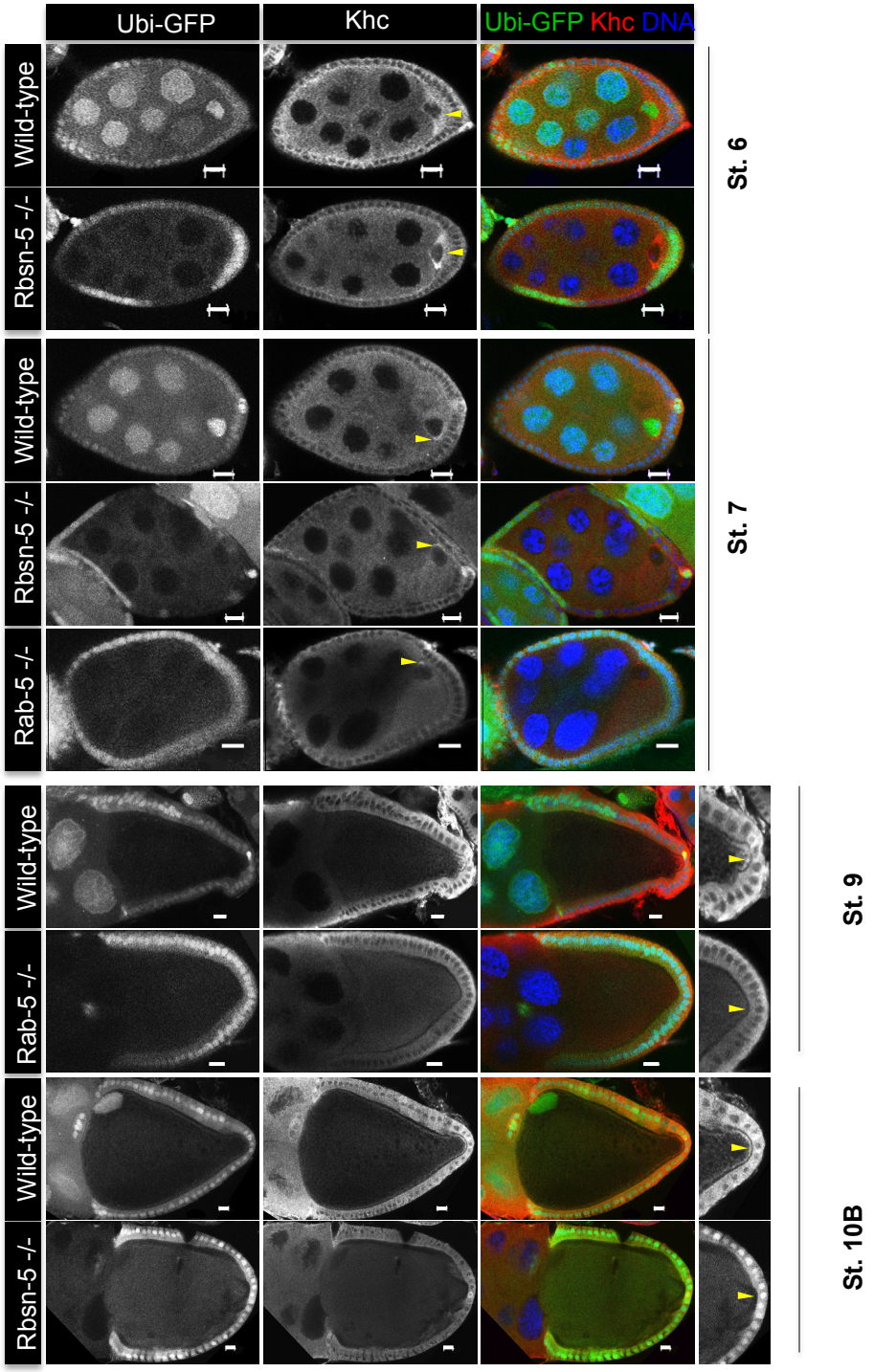

Supplementary Material S4:

Oocyte microtubule polarity is not affected during early oogenesis in *Rab5* and *Rbsn-5* mutants. *Rab5*^{2} and *Rbsn-5*^{C241} germline clones were generated and stained with anti-Khc antibodies (red). Mutant clones are marked by the absence of GFP (green). Accumulation of Khc (arrowheads) is only affected in mutant egg chambers from stage 9 on when the signal becomes fainter at the posterior cortex (arrowheads in the magnification). Ovarioles were also stained with Hoechst (blue) to visualize the DNA. Scale bars: 10 µm.